HHS Public Access

Author manuscript

Nature. Author manuscript; available in PMC 2022 July 04.

Published in final edited form as:

Nature. 2021 May ; 593(7857): 114–118. doi:10.1038/s41586-021-03413-6.

An amygdala circuit that suppresses social engagement

Jeong-Tae Kwon[1,2], **Changhyeon Ryu**[1,2,†], **Hyeseung Lee**[1,2,4,†], **Alec Sheffield**[1,2], **Jingxuan Fan**[2], **Daniel H. Cho**[2], **Shivani Bigler**[2], **Heather A. Sullivan**[3], **Han Kyung Choe**[2], **Ian R. Wickersham**[3], **Myriam Heiman**[1,2,4], **Gloria B. Choi**[1,2,*]

[1]Picower Institute for Learning and Memory, Massachusetts Institute of Technology, Cambridge, MA 02139, USA.

[2]Department of Brain and Cognitive Sciences, Massachusetts Institute of Technology, Cambridge, MA 02139, USA.

[3]McGovern Institute for Brain Research, Massachusetts Institute of Technology, Cambridge, MA 02139, USA.

[4]Broad Institute of MIT and Harvard, Cambridge, MA 02142, USA.

Abstract

Innate social behaviors, such as mating and fighting, are fundamental to animal reproduction and survival[1]. However, social engagements can also put an individual at risk[2]. Little is known about the neural mechanisms that allow for appropriate risk assessment and the suppression of hazardous social interactions. We have identified the posteromedial nucleus of the cortical amygdala (COApm) as a locus required for the suppression of male mating when a female is sick. Using anatomical tracing, functional imaging, and circuit-level epistatic analyses, we show that suppression of mating with an unhealthy female is mediated by the COApm projections onto the glutamatergic population of the medial amygdalar nucleus (MEA). We further show that the role of the COApm to MEA connection in regulating male mating behavior relies on the neuromodulator thyrotropin-releasing hormone (TRH). TRH is expressed in the COApm while the TRH receptor (TRHR) is found in the postsynaptic MEA glutamatergic neurons. Manipulating neural activity of TRH-expressing neurons in the COApm modulated male mating behavior. In the MEA, activation of the TRHR pathway, by ligand infusion, inhibited mating even towards healthy females, while genetic ablation of TRHR facilitates mating with unhealthy individuals. We have, therefore, uncovered a novel neural pathway that relies on the neuromodulator TRH to modulate social interactions according to the health status of the reciprocating individual. An individual is in need to balance the cost-benefit of social interactions, with deficits in the ability to select healthy mates likely leading to the spread of disease.

*Correspondence and requests for materials should be addressed to G.B.C. (gbchoi@mit.edu).

†These authors contributed equally to this work

Author Contributions

J.K. and G.B.C. conceptualized the study. J.K., H.L., C.R., M.H. and G.B.C. designed the experiments and/or provided advice and technical expertise. J.K., H.L., C.R., A.S., J.F., D.H.C., S.B., H.S., H.K.C. performed the experiments. I.R.W. provided reagents. J.K. and G.B.C. wrote the manuscript with inputs from the co-authors.

Supplementary Information

Supplementary statistical information is attached.

The authors declare no competing financial interests.

Social behaviors are fundamental for survival—for the individual as well as the species. Social engagements, however, also carry inherent risks, such as contracting pathogens from a sick mate[2]. Thus, the ability to modify innate social behaviors to account for the health status of a partner is essential to minimize potential risks and to enhance survival[3–5]. Innate social behaviors, such as mating and aggression[1], are largely thought to be coordinated by developmentally determined neural pathways[6–9]. However, the molecular and neural circuit mechanisms that mediate the adaptive modulation of innate social interactions according to the health of a partner are still lacking.

Males avoid mating with unhealthy females

Mice avoid a potentially sick partner. When we presented male mice with a pair of estrus females, they preferentially mounted females that were intraperitoneally injected with control phosphate-buffered saline (PBS-female) over those injected with lipopolysaccharide (LPS-female), a cell wall component of gram-negative bacteria that induces an immune state that mimics bacterial infection[10] (Extended Data Fig. 1a–b). No such bias was observed when males were given a choice between two untreated healthy females (Extended Data Fig. 1c). We observed no preference for PBS- or LPS-females in a three-chamber sociability assay in which females are encaged in wired cups (Extended Data Fig. 1d), suggesting that direct access to the female is likely needed to establish her health status. To further examine the repertoire of male mating behaviors displayed towards unhealthy females, we carried out a single-female assay, in which males were presented either with a PBS- or LPS-female (Fig. 1a and Extended Data Fig. 1e). Males reduced the amount of anogenital investigation towards LPS-females, while maintaining a comparable level of facial investigation (Extended Data Fig. 1e–f). Notably, the percentage of male mice that mounted LPS-females as well as the duration and frequency of mounting bouts were reduced, while the latency to mount LPS-females substantially increased (Fig. 1b–e). These observations indicate that males lessen the expression of mating behaviors toward LPS-treated, unhealthy females. Of note, the LPS treatment induced changes also in the repertoire of female behaviors, generally reducing locomotion as quantified by the total number of cage crossings (Extended Data Fig. 1g,h).

COApm is activated by unhealthy females

We next carried out experiments using the single-female assay to elucidate the molecular and circuit-level mechanism underlying the suppression of male mating behavior towards unhealthy, LPS-females. We reasoned that brain regions that play a role in suppressing mating may be specifically activated in the presence of LPS-females. Consistent with the role of the accessory olfactory system in recognizing the health of other individuals[11–14], we found that surgically removing the vomeronasal organ impaired active suppression of male mating behaviors towards LPS-females (Extended Data Fig. 2a). Therefore, using FOS expression as a marker of neural activity, we examined whether the accessory olfactory bulb (AOB) and its direct downstream targets —the bed nucleus of the stria terminalis (BST), MEA, and COApm[15,16] (Extended Data Fig. 2b–d)—are preferentially active when a male is presented with an LPS-female compared to a PBS-female. We observed the highest

fold change in the number of FOS+ neurons in the COApm and, to a lesser extent in the AOB and the posteroventral portion of the MEA (MEApv) (Fig. 1f,g and Extended Data Fig. 2h). To directly monitor COApm neural activity in awake behaving animals, we expressed the genetically encoded fluorescent calcium indicator GCaMP6s and performed fiber photometry (Fig. 1h). While direct investigation of both PBS- and LPS-females evoked time-locked neural activity in the COApm, the response to LPS-females was more pronounced and did not readily habituate when compared to PBS-females (Fig. 1i–l and Extended Data Fig. 3a–c). Levels of neural activity in the COApm during investigation, therefore, negatively correlated with the incidence of mounting (Fig. 1m). Notably, the COApm remained silent during mounting (Fig. 1n,o). We did not find any observable difference in COApm neural activity (Extended Data Fig. 3d,e) or males' mounting attempts (Extended Data Fig. 3f–i) towards estrus versus diestrus females during a 10-min testing period. A higher percentage of estrus female partners, however, were found with mating plugs 24-hr after the testing (Extended Data Fig. 3j), demonstrating their enhanced receptivity compared to diestrus females. These data collectively indicated that COApm is selectively activated by the unhealthy status of reciprocating females independently of their estrus phase.

COApm is a direct target of the AOB (Extended Data Fig. 2b–g) suggesting that the suppression of mating behaviors induced by LPS-females might be dependent on non-volatile odorants. We thus used urine and feces of LPS-females as odor sources to test if odor alone can substitute for an LPS-female. Indeed, LPS-odor induced a greater number of FOS+ neurons in the COApm than PBS-odor (Extended Data Fig. 4a–c). A similar observation was made using fiber photometry (Extended Data Fig. 4d,e). LPS-odor painted on healthy females resulted in a decrease in both mounting and anogenital investigation of otherwise healthy females (Extended Data Fig. 4f–k). Importantly, LPS-odor suppressed male mating behaviors but did not alter the behaviors of the odor-presenting females (Extended Data Fig. 4l,m), demonstrating that suppression of male sexual behaviors depends largely on the olfactory bouquet of the female rather than the behavioral changes that follow LPS treatment.

COApm suppresses male mating

The observation that COApm preferentially responds to LPS-females while remaining silent during mounting suggested that it might be directly involved in suppressing male mating behaviors in the presence of unhealthy partners. Consistent with this notion, optogenetic activation of COApm neurons robustly inhibited mounting even towards healthy females (Fig. 2a–e, Extended Data Fig.5a). COApm photoactivation, however, did not affect the total investigation time directed towards females (Extended Data Fig. 5b) or the expression of other motivational behaviors, such as feeding and sociability (Fig. 2f,g). Mice also showed neither aversion nor attraction for the side of the chamber where COApm was activated during a real-time place preference test (RTPP) (Fig. 2h). We noted that COApm photoactivation increased self-grooming. However, this increase could at best account for a small fraction of the total reduction in mounting, and the fidelity with which the COApm stimulation induced grooming was low (Extended Data Fig. 5c,d). In accord with the results from the photoactivation experiments, inhibition of the COApm via bilateral expression of

the inhibitory DREADD hM4Di (Fig. 2i and Extended Data Fig. 5e) significantly increased male mounting behavior towards LPS-females, with male mice exhibiting both heightened duration and frequency of mounting (Fig. 2j–l and Extended Data Fig. 5g–j). The latency to the first mounting attempt showed a trend towards a decrease, although the duration of direct investigation remained unchanged (Fig. 2m and Extended Data Fig. 5f,k). Inhibition of COApm did not affect mounting towards untreated, healthy females regardless of the phase of the estrus cycle (Extended Data Fig. 5l–u). Taken together, these results demonstrate that the COApm has a critical role in the suppression of mating behaviors when male mice are faced with unhealthy females.

Suppression of mating engages the MEA

To gain further insights into the circuit-level mechanisms that underlie COApm suppression of social behaviors, we performed anterograde tracing experiments to identify downstream targets of the COApm. Among the labeled regions, the MEA, known to be involved in regulating innate social behaviors[17–20], receives the largest COApm axonal projection (Extended Data Fig. 6a,b). The majority of MEA neurons postsynaptic to the COApm are located in the MEApv, which is enriched for Vglut2(+) glutamatergic neurons over Vgat(+) GABAergic neurons (Extended Data Fig. 6c–g). We confirmed the functional relevance of the COApm-to-MEA$^{Vglut2+}$ projection by monitoring the activity of the Vglut2(+) or Vgat(+) populations in response to optogenetic activation of the COApm. Stimulating the COApm evoked responses preferentially in MEA-Vglut2(+) neurons as measured using both GCaMP fluorescence (Fig. 3a–e). Moreover, MEA-Vglut2(+) neurons, like the COApm, were directly activated by LPS-females (Extended Data Fig. 6h,i). These data suggest that the COApm suppresses mating behavior towards LPS-females by engaging the MEA-Vglut2(+) population. Indeed, optogenetic stimulation of the COApm axonal terminals in the MEA inhibited mating (Fig. 3f) similarly to the stimulation of COApm neuronal cell bodies (Fig. 2a–e). Activation of the MEA-Vglut2(+) population also suppressed mating behavior (Fig. 3g). Conversely, inhibiting the MEA-Vglut2(+) population impaired the natural ability of the males to suppress mating towards an unhealthy LPS-female (Fig. 3h). Furthermore, using circuit-level functional epistasis experiments, we demonstrated that activation of the COApm axonal terminals, while concurrently inhibiting the MEA-Vglut2(+) population, fails to suppress mating behavior (Fig. 3i, also see Extended Data Fig. 7), suggesting that the COApm-to-MEA$^{Vglut2+}$ projection is required to modulate male mouse mating behaviors on the basis of the perceived health status of the female.

Suppression of mating engages TRH-TRHR

Determining the distinctive transcriptional profile of COApm neurons may provide insight on the genetic basis that allow the COApm to regulate social interactions. To this end, we used viral strategies[21] to label the subset of COApm neurons that specifically project to the MEA-Vglut2(+) neurons, with a GFP-tagged version of the ribosomal protein L10a (Extended Data Fig. 8a). Following Translating Ribosome Affinity Purification (TRAP)[22], we performed RNA sequencing and differential gene expression analyses, identifying 1242 differentially expressed genes that are highly enriched in the COApm population that projects to MEA-Vglut2(+) neurons (Extended Data Fig. 8b). Of those, we selected the

tripeptide molecule thyrotropin-releasing hormone (TRH) - one of the most highly enriched candidates belonging to the neuroactive ligand-receptor interaction pathway - for further analyses (Extended Data Fig. 8c). *In situ* hybridization confirmed that *Trh* is specifically and selectively expressed in the COApm (Fig. 4a,b). We next functionally tested the role of COApm-TRH(+) neurons in suppressing male mating behaviors. Selective activation of TRH(+) neurons robustly suppressed mounting towards healthy females (Fig. 4c–h). On the other hand, photostimulation of TRH(−) cells did not suppress mounting behavior, indicating that the ability to modulate mating is restricted to TRH(+) neurons in the COApm (Extended Data Fig. 9a–g). While *Trh* is expressed by COApm neurons, the TRH receptor (TRHR) is selectively enriched in Vglut2+ MEA neurons (Fig. 4i,j), suggesting that TRH may modulate expression of innate social behaviors by acting on the COApm-MEA$^{Vglut2+}$ circuit. Consistent with this hypothesis, direct delivery of the TRHR agonist taltirelin[23] into the MEA evoked robust responses in Vglut2+ neurons *in vitro* (Extended Data Fig. 9h–l) and suppressed mating towards healthy females (Fig. 4k–o and Extended Data Fig. 9m). To determine whether TRHR signaling in the MEA is involved in modulating mating behaviors according to the health status of females, we generated a TRHR conditional knock-out mouse line (Extended Data Fig. 10a). Genetic removal of the TRHR, by delivering Cre-expressing virus into the MEA, reduced neural activity evoked by photoactivation of COApm-MEA projections (Extended Data Fig. 10b–g) and impaired a male's ability to suppress mating towards LPS-females (Fig. 4p–t). These data collectively indicate that suppression of mating behavior towards an unhealthy mate depends on the activity of the COApm-MEA$^{Vglut2+}$ projection expressing TRH-TRHR.

Discussion

While an increasing number of studies suggests that sick individuals engage in a repertoire of sickness behaviors to limit their social interactions[24–27], little is known about how healthy individuals respond to an infected conspecific. Here, we have identified an amygdalar circuit responsible for discouraging innate reproductive social behaviors if a male encounters a sick partner. We show that the odor bouquet of a sick female is sufficient to activate the COApm and inhibit male mating behaviors, suggesting odorants associate with the "sickness state" of the females can be smelled by males, using odorant receptors like the family of the formyl peptide receptors[12,13]. Posteroventral MEA-Vglut2(+) neurons, postsynaptic to the COApm, are essential for the modulation of mating behaviors to unhealthy females. The posterodorsal MEA-Vglut2(+) neurons have been previously shown to have a similar role in inhibiting innate social behaviors[17,20], suggesting that Vglut2(+) neurons in the dorsal and ventral parts of the posterior MEA could comprise a functional unit partaking in the regulation of social behaviors. Our data also suggest that the COApm-MEA$^{Vglut2+}$ projection relies on TRH to modulate reproductive social behaviors. Of note, thyroid dysfunction and dysregulated levels of thyroid hormones have been associated with depression and social anxiety in humans[28,29]. Whether TRH has a role in the expression of these symptoms remains to be explored. Overall, our data characterized a novel neural node that takes into account the health status of the interacting partner to modulate innate mating behavior. As limiting the spread of a pathogen likely requires the concerted efforts of both infected and uninfected individuals, the COApm-MEA$^{Vglut2+}$ circuit we have identified is likely to

contribute to the wellness of an individual as well as its community. It is of paramount importance for an individual to maintain a balance between the drive to socially interact while minimizing risks through social avoidance.

Methods

Animals

All experiments were performed according to the Guide for the Care and Use of Laboratory Animals and were approved by the National Institutes of Health and the Committee on Animal Care at Massachusetts Institute of Technology. C57BL/6J (000664), Slc32a1(Vgat)-Cre (028862), Slc17a6(Vglut2)-Cre (016963), and Ai14 (007914) were purchased from Jackson Laboratories and inbred. Generation of Trh-IRES-Cre was described[30]. In order to develop a conditional knockout mouse line that removes TRHR in a Cre-dependent manner, a targeting vector with two loxP sites flanking common exons 1 and 2 was generated using the CRISPR/Cas9 system (Biocytogen). For PCR genotyping, the following primers were used (EGE-WFZ-023-5'loxp-F 5'-GTTCTGATGCCCAGATGGTCCTGTC-3', EGE-WFZ-023-5'loxp-R 5'-TGCAGTCCCCAGGGCTTGAGATAAA-3' for WT 301bps/Floxed 378bps and EGE-WFZ-023-3'loxP-F 5'-ACTGAGTGTGCTTTTAGAACCATGT-3', EGE-WFZ-023-3'loxP-R 5'- TTTGGTTAATGGCCAGCTACACCTT-3' for WT 342bps/Floxed 415bps). Mice were housed with 20–22°C, 40–60% humidity and a 12-hour light cycle and given ad libitum access to food and water. All mice were males aged 2–5 months unless otherwise specified.

Stereotaxic surgery

Surgeries were carried out using aseptic techniques. Mice were anaesthetized using a mixture of ketamine (100 mg/kg, intraperitoneal injection) and xylazine (10 mg/kg, intraperitoneal injection). Mice were given preoperative slow-release buprenorphine (1.0 mg/kg, subcutaneous injection). Injection coordinates from bregma in mm: COApm, ±2.9 ML, −2.9 AP, −5.7 DV; MEApv, ±2.1 ML, −1.7 AP, −5.6 DV; MEApd, ±2.2 ML, −1.7 AP, −5.4 DV; AOB, +1.0 ML, +4.25 AP, −1.8 DV with a 20-degree angle relative to AP. Injections were performed using a pulled fine-glass capillary at 0.1μl/min, 1μl total for Cre-dependent viruses and 0.4μl otherwise. For fiber photometry, AAV1-Syn-GCaMP6s or AAV1-Syn-FLEX-GCaMP7f (Penn Vector Core)[31] were delivered to COApm of wild-type mice or MEA of Vglut2-Cre mice, respectively, in the right hemisphere with a 400-μm diameter optic fiber implanted 300μm above the injection targets. For experiments involving optical stimulation[32], wild-type or Vgat/Vglut2/Trh-Cre mice received bilateral stereotaxic injections of AAV2-hSyn-hChR2-EYFP (UNC Vector Core) or AAV2-Ef1α-DIO-hChR2-EYFP (UNC Vector Core), respectively, with 300-μm optic fibers implanted 200μm above the injection targets. Control groups were injected with AAV2-hSyn-EYFP or AAV2-Ef1α-DIO-EYFP, respectively, with optic fibers implanted similarly. For photoactivation of COApm-MEA projections, wild-type mice received bilateral injections of virus (AAV2-hSyn-hChR2-EYFP) to COApm with optic fibers implanted in MEA. For MEA fiber photometry with COApm photoactivation, Vgat/Vglut2-Cre mice received unilateral injections of virus encoding ChrimsonR (AAV2-hSyn-ChrimsonR-tdTomato (UNC)) to COApm and virus encoding GCaMP6s (AAV1-

CAG-Flex-GCaMP6s) to MEA. A 300-μm optic fiber was implanted in COApm for photoactivation and a 400-μm optic fiber was implanted in MEA for fiber photometry. Optic fibers were prepared in-house as described previously[33]. For photoactivation of AOB, wild-type mice received unilateral injection of AAV2-hSyn-hChR2-EYFP to AOB. For photoactivation of TRH(−) cells, Trh-Cre mice received unilateral injection of AAV1/2-Ef1a-DO-hChR2-mCherry (Addgene #370820) to COApm. Control group was injected with AAV1/2-Ef1a-DO-DIO-TdTomato-EGFP (Addgene #37120). For DREADD inhibition experiments[34], wild-type or Vglut2-Cre mice received bilateral stereotaxic injections of AAV2-hSyn-hM4D(Gi)-mCherry (Addgene) or AAV2-hSyn-DIO-hM4D(Gi)-mCherry (Addgene), respectively, either in COApm or MEA. AAV2-hSyn-mCherry or AAV2-hSyn-DIO-mCherry were used for control groups, respectively. For administration of taltirelin into MEA, guide cannulas (26 gauge, PlasticsOne) were implanted 500μm above the MEA (±2.2 ML, −1.7 AP, −5.1 DV). Guide cannulas were fitted with dummy cannulas to maintain cannula patency after surgery. For genetic removal of Trhr in the MEA, wild-type or homozygous Trhr conditional knock-out mice ($Trhr^{fl/fl}$) received bilateral injection of AAV_1-hSyn-GFP or AAV_1-Syn-Cre in the MEA. Removal of the vomeronasal organ was performed as previously described[35]. Briefly, mice were anesthetized and the lower jaw was gently opened and fixed with a homemade mouth holder. A midline incision was made in the soft palate and the underlying bone was exposed. The rostral end of the VNO was exposed and bilaterally removed. The resulting cavity was filled with a gel foam and the incision was closed with absorbable sutures. All animals recovered for at least one week before behavioral testing.

Virus preparation

Chimeric AAV_1/AAV_2[36] viruses were prepared with plasmids for pAAV-Ef1a-DO-hChR2-mCherry (Addgene #370820) and pAAV-Ef1a-DO-DIO-TdTomato-EGFP (Addgene #37120). Briefly, AAV plasmids, AAV1/AAV2 Rep/Cap, and adenovirus-helper plasmid (pFdelta6) were transfected into HEK293FT cells and incubated for 3 days. Cells were lysed and rAAVs harvested by centrifugation to remove cellular debris. Finally, rAAVs were purified using heparin columns.

Tissue slice preparation and immunohistochemistry

Mice were transcardially perfused with cold paraformaldehyde (PFA) (4% in PBS). Brains were kept in PFA overnight at 4 °C before vibratome sectioning (Leica VT1000s). Brains were cut at 50-μm thickness for FOS immunohistochemistry. Brains were cut at 100-μm thickness for all other experiments. Sections were incubated in blocking solution (0.4% Triton X-100 and 2% goat serum in PBS) for 30 min. Sections were then incubated in blocking solution containing rabbit anti-FOS (1:500, Millipore, ABE457) primary antibody overnight at room temperature. Sections were washed in wash buffer (0.4% Triton X-100 in PBS) three times and incubated in blocking solution containing Alexa 488 Goat anti-rabbit (1:250, Life Technologies, A11034) secondary antibodies and DAPI (1:5,000, D1306, Thermo Fisher) for two hours at room temperature. Images of stained slices were acquired using confocal microscopes (LSM710 and LSM900, Carl Zeiss) with a 10×, 20× or 40× objective lens.

Anatomical tracing

For anterograde tracing of COApm axonal projections, wild-type mice received unilateral stereotaxic injections of virus (AAV_2-hSyn-tdTomato) into COApm. 4 weeks later, mice were sacrificed and 100-μm thick coronal brain slices were prepared. Images were taken from brain regions expressing tdTomato every 300-μm using a confocal microscope (LSM710, Carl Zeiss). Using Zen software (Carl Zeiss), regions of interest were defined based on the Paxinos brain atlas[37] and total fluorescence intensity in each region was calculated. For anterograde trans-synaptic tracing, AAV1-hSyn-Cre (0.5μl) virus was injected into AOB in Ai14 reporter mice that express tdTomato in a Cre-dependent manner. After two weeks, mice were sacrificed and coronal brain sections were prepared of BST (AP: 0.2~−0.4), MEA (AP: −1.2~−2.1) and COApm (−2.4~−3.2). Images were taken every 200-μm using a confocal microscope (LSM710, Carl Zeiss) and the number of tdTomato positive cells were manually counted. For anterograde trans-synaptic tracing of COApm, the same histological and imaging procedures were used for MEA (~AP-1.7).

Quantification of FOS (+) cells

For FOS expression studies after interaction with healthy or sick females, subject male mice were co-housed with a female for 3 days for habituation. The female was separated and intraperitoneally injected with either PBS or LPS and 2 hours later returned to the male cage. Males were sacrificed 90 min after a 2-min free interaction with the female and brains were processed for immunohistochemical detection of FOS protein. All cells were counted bilaterally from two coronal sections of each respective brain region, as defined by the Paxinos brain atlas[37]. Regions quantified include: AOBmi: mitral layer of the accessory olfactory bulb, AOBgr: granular layer of the accessory olfactory bulb, BST: bed nucleus of the stria terminalis, MEApd: posterodorsal part of the medial amygdalar nucleus, MEApv: posteroventral part of the medial amygdalar nucleus, COApm: posteromedial nucleus of the cortical amygdala. For FOS expression studies after interaction with PBS- or LPS-odor, males were sacrificed 90 min after a 2-min exposure to urine and feces obtained from females intraperitoneally injected with PBS (PBS-odor) or LPS (LPS-odor) and brains were processed for immunohistochemical detection of FOS protein in the COApm. For FOS expression studies after photoactivation, males were sacrificed 90 min after photoactivation of AOB or COApm and brains were processed for immunohistochemical detection of FOS protein in the COApm.

Fiber photometry

The fiber photometry system was built as previously described[38]. Briefly, blue light from a 473 nm diode laser (Company, USA) was chopped at 197 Hz and reflected off of a dichroic mirror (FF495, Semrock, NY, USA) and coupled into a 600μm optical fiber patch cord (0.48NA, Thorlabs, BFH48–600) through a microscope objective (40 × 0.65 NA, Olympus). The patch cord was coupled with a free optic fiber, which has the same light efficiency as the implanted one, and light power at the fiber tip was set to 20μW. The patch cord was connected to an implanted 400μm optical fiber via a ceramic sleeve. GCaMP6s fluorescence was collected through a bandpass filter (FF01-520/35) into a photodetector (2151, NewFocus). The signal was passed through a lock-in amplifier (Model SR810,

Stanford Research Systems, CA, USA) and digitized and collected with a LabVIEW DAQ (100Hz sampling frequency, LabVIEW), and recorded by custom LabVIEW software. Animal behavior was recorded using EthoVision XT tracking system (Noldus, Wageningen, Netherlands) and time-stamped with photometry data using the LabVIEW TTL pulse. Male mice expressing GCaMP in COApm or MEA were single housed and habituated with fiber coupling in their home cage placed in the behavior chamber for 30 min. During this habituation, the fluorescence signal level was checked and the mice showing basal fluorescence level between 3–5 amplitudes were used for further experiments to minimize the signal intensity variation between animals, which might be caused by variable GCaMP expression levels and optic fiber placements. A stimulus mouse (PBS- or LPS-females in estrus; estrus or diestrus healthy females; healthy females painted with PBS- or LPS-odor) or stimulus odor (PBS- or LPS-odor) were presented for 10 min in sequential and counterbalanced sessions with an 1h-interval in between the sessions. Urine and feces from PBS- or LPS-females served as PBS- or LPS-odor. The raw fluorescence signal was normalized to the mean of the 1-min baseline prior to the first contact for z-score calculation. The mean z-score of fluorescence during direct investigation was calculated from the first 3-min periods. For the generation of the heat map, z-scored fluorescence signals were further min-max normalized.

Behavioral analyses

All behavior experiments were performed between three hours before and after light offset time (light offset: 7:00pm). Mice were transferred to the testing area at least three hours before the initiation of experiments. Tracking of mouse behavior was done using the EthoVision XT (Noldus, Wageningen, Netherlands) tracking system.

Mating assays.—Naive C57BL/6J females were used. All females were in estrus, unless otherwise indicated to be in diestrus. Estrus phase was checked by vaginal smear on the testing day[39]. Male mice were first screened for mounting behavior. After 30-min of habituation, they were presented with a female in its home cage for 5 min. Only the males that mounted the female within the first 5 min period were used for experimentation. Males that successfully mounted were then single-housed for a minimum of three days prior to the behavior test. For testing, the home-cage of a male mouse was placed in a behavioral chamber with recording capabilities with a side view camera. After a 10 min acclimation in the behavioral chamber, an intruder female was placed into the male's home cage for 10 min before being removed. Only for the experiments described in Extended Data Fig. 1a–c, two females were simultaneously introduced. Intruder females were either untreated, or intraperitoneally injected with PBS (PBS-female) or LPS (LPS-female, 0.5mg/kg) 2 hours before testing, or painted with urine and feces from PBS-females (PBS-odor) or LPS-females (LPS-odor). Male mounting attempts (percent males engaged in mounting, mounting time, number of mounts, and latency to the first mounting attempt), investigation (sniffing of facial or anogenital regions), and social or self-grooming were manually scored. Four different categories of female behaviors (Run: the display of an active escaping behavior from males' mounting attempts; Rear up: the display of a defensive posture by facing up against the male during mounting attempts; Sit: the display of a passive, non-receptive response by sitting down and not exposing the genital region during males'

mounting attempts; Lordosis: the display of receptive responses, including the canonical lordosis posture with the curved spine and a standing posture with four limbs without the curved spine, that allow for males mounting) displayed upon males' mounting attempts were manually scored. For the behavioral raster plots shown in Extended Data Figure 1i, female behaviors during the rest of the interactions were also analyzed and these include exploration of the cage, which is a novel environment to the females (e.g. sniffing and digging), and a sitting posture. The presence of mating plugs in females was determined 24 hours following the mating assay to estrus versus diestrus females, in which the females stayed with the males after the 10-min test.

Mating assays with optogenetic activation.—ChR2, EYFP or tdTomato was virally targeted to COApm, COApm-TRH(+), COApm-TRH(−) or MEA-Vglut2(+) and optic fibers were bilaterally implanted. Mice were habituated for fiber coupling a day before testing. On the testing day, an optic cable was connected to the optic fiber to deliver 405 nm laser stimulation. After a 10-min acclimation, a female was placed in the subject's home cage. Mice behavior was monitored through a side-view camera and a 10-sec photoactivation (2mW, 20Hz square wave, 10ms pulse width) was manually triggered at each instance of contact investigation.

Mating assays with DREADD inhibition.—Male mice expressing hM4Di or mCherry in COApm or MEA-Vglut2(+) were habituated for intraperitoneal injection a day before testing in the testing room. On the testing day, Clozapine N-Oxide (1 mg/kg) was diluted in sterile saline and intraperitoneally administered to male mice 40 min prior to testing.

Mating assays with concurrent photoactivation of COApm-MEA projections and DREADD inhibition of MEA-Vglut2(+) neurons.—Experimental group mice were Vglut2-Cre male mice bilaterally expressing ChR2 in COApm and hM4Di in MEA-Vglut2(+) neurons with optic fibers implanted in MEA. Control group mice were Vglut2-Cre mice expressing ChR2 in COApm and mCherry in MEA-Vglut2(+) neurons. Clozapine N-Oxide (1mg/kg) was diluted in sterile saline and administered to male mice 40 min prior to testing. Photoactivation of COApm-MEA projections was manually triggered at each instance of contact investigation.

Mating assays with Taltirelin injection to MEA. Wild-type male mice with guide cannulas implanted in MEA were habituated for injection cannula insertion a day before testing. On the testing day, mice were briefly anesthetized using isoflurane, and either vehicle or Taltirelin (10 ng/side in 0.5 μl at a rate of 180 nl/min, 7956-ML/CF, R&D) was administered bilaterally into the MEA through 500-μm projecting injector tips (PlasticsOne). Mice were returned to the home cage and placed in a behavioral chamber. 20 min after administration of vehicle or taltirelin, mice were assayed for mating behavior. Cannula placements were histologically verified.

Feeding assay.—Male mice expressing ChR2 in COApm were single-housed and food-deprived for 12 hours. Mice were then connected to optic fibers and placed back in their home cage. Following 10 min, a single pre-weighed food pellet was placed in the center of their home cage. The amount of time spent eating was measured over a ten-minute

period, and the pellet was removed and re-weighed to calculate the amount of food eaten. Photoactivation of COApm (2 mW, 20 Hz square wave, 20 % duty cycle) occurred throughout the 10-min testing period.

Three-chamber social approach assay. Single-housed male mice expressing ChR2 in COApm were assayed for sociability using a three-chamber social approach assay. The arena was constructed of white acrylic (50 cm × 35 cm × 30 cm). Wire cups (Spectrum Diversified) were placed in the back left and right corner of the arena beneath water-filled 1-L bottles (Nalgene). On day 0, mice were habituated to the arena for 20 min and returned to their home cage. On day 1, mice were connected to optic fibers and placed in the center of the arena and allowed to freely explore. Following 10-min of habituation, mice were confined to the center of the arena. An inanimate object (rubber stopper) or a male conspecific were placed beneath the wire cups. Placement of the inanimate object and social target were alternated. Mice were then allowed to freely explore the arena for 10 min. During this period, photoactivation of COApm (2 mW, 20 Hz square wave, 20% duty cycle) was automatically triggered during interaction with either the inanimate object or social target. Interaction time was defined as time spent in the areas circumscribing the wire cups (<2 cm). Sociability was defined as interaction time with the social target divided by total interaction time and expressed as a percentage.

Three-chamber social preference assay.—Single-housed wild-type mice were used for the behavioral assay as described above (“Three-chamber social approach assay”), except the target objects were PBS- and LPS-females.

Real time place preference.—Male mice expressing ChR2 in COApm were assayed for preference of COApm photoactivation in a real time place preference (RTPP) assay. The arena consisted of two chambers constructed of white acrylic (30cm × 30cm). Mice were connected to optic fibers and placed in the left chamber. Photoactivation of COApm (2 mW, 20 Hz square wave, 20% duty cycle) was triggered whenever the mouse entered the right chamber. Stimulation preference was defined as the time spent in the chamber paired with photoactivation divided by total trial duration (10 min) and displayed as a percentage.

In situ hybridization

Fluorescence in situ hybridization (FISH) was conducted with ACDBio RNAscope Multiplex Fluorescence Assay. Following probes were used: C1: Trhr (Mm-Trhr: 443771), C2: Vglut2 (Mm-Slc17a6-C2: 319171-C2), C3: Vgat (Mm-Slc32a1-C3: 319191-C3); C1: Trh (Mm-Trh: 436811). Brain tissues were obtained from age-matched 8–10 week-old sexually naïve male C57BL/6J mice and immediately fresh-frozen in optimal cutting temperature (OCT) medium on dry ice. Twenty-micrometer sections were obtained using a cryostat (Leica, Germany) and stored at − 80 °C. RNAscope procedures were performed according to the user manual provided by ACDBio with modifications specified as following. Briefly, sections were fixed with 4% chilled paraformaldehyde (PFA) for 15 min and washed in 1 × phosphate-buffered saline (PBS) twice for 2 min each. Sections were then dehydrated consecutively in 50%, 75%, 100%, and 100% ethanol for 5 min each. Tissue was digested with Protease IV for 13 min at room temperature and washed twice in

1 × PBS with agitation. Vglut2 and Vgat probes were diluted 1: 50 in Trhr probe solution and pipetted onto each slide. Probe hybridization was conducted for 2 h and 30 min at 40 °C and slides were then washed in 1 × wash buffer twice for 4 min each. Sections were then incubated at 40 °C in Amp1 for 35 min, Amp2 for 17 min, Amp3 for 35 min, and Amp4 for 17 min, with two 1 × Wash Buffer rinses between each incubation. Sections were finally treated with DAPI for 30 sec, mounted with CC/Mount and stored at 4 °C. Images were acquired using Zeiss LSM 710 and LSM900 confocal microscopes (x40 objective, 1.2 NA) and a Zeiss Axio Imager.Z2 microscope (x10 objective, 0.45 NA). Imaging settings were established during the first acquisition and not modified afterwards. Target genes (*Trh, Trhr, Vgat, and Vlut2*) and DAPI expression were quantified using QuPath[40]. For *Trh* quantification, cells were divided into the following categories based on level of *Trh* expression: low = 1–3 puncta, medium = 4–9 puncta, high = 10–15 puncta, highest = >15 puncta. For co-expression of *Vglut2*, *Vgat* and *Trhr*, cells were classified as positive if the level of target expression was > 3 puncta. Percentage of co-expression is calculated as the number of *Vglut2* and *Trhr* or *Vgat* and *Trhr* double positive cells divided by the total number of Trhr positive cells. For validation of conditional knock-out of Trhr in the MEA, Trhr probe was used on brain tissues from $Trhr^{fl/fl}$ animals, which received stereotaxic injections of AAV_1-Syn-Cre in MEApv. $Trhr^{fl/fl}$ animals without virus injection served as a control. To quantify the percentage of MEApv neurons expressing *Trhr*, cells were classified as Trhr-positive if the level of target expression was >1 puncta.

Calcium imaging of MEA brain slices

Slice preparation. Virus (AAV_1-Syn-FLEX-GCaMP7f) was bilaterally delivered to MEA of vGlut2-Cre mice. 4–8 weeks after the virus injection, mice were anesthetized with isoflurane. Before decapitation, intracardiac perfusion was performed with an ice-cold cutting solution containing (in mM): 96 N-Methyl-D-glucamine (NMDG), 2.5 KCl, 10 MgSO4, 0.5 CaCl2, 1.25 NaH2PO4, 25 NaHCO3, 25 glucose, 17.5 HEPES, 5 Na ascorbate, 2 thiourea, 3 Na pyruvate, 12 L-acetyl-cysteine, perfused with 95% O_2 and 5% CO_2 (pH 7.3–7.4 adjusted by HCl after bubbling). Coronal slices of the MEA (300 μm thick) were obtained by a vibratome (VT1200s, Leica) in the ice-cold cutting solution. The slices were immediately transferred to the same cutting solution at 34 °C for 10 min, and then transferred to slice holding solution at room temperature containing (in mM): 94 NaCl, 2.5 KCl, 2 MgSO4, 2 CaCl2, 1.25 NaH2PO4, 25 NaHCO3, 25 glucose, 14 HEPES, 5 Na ascorbate, 2 thiourea, 3 Na pyruvate, 12.3 L-acetyl-cysteine, perfused with 95% O_2 and 5% CO_2 (pH 7.3–7.4 adjusted by NaOH after bubbling). The slices were recovered in the holding solution for a minimum of 1.5 hours. All experiments were done within 6 hours from the start of the recovery.

Image acquisition and data analysis. Slices were transferred from the holding solution to an immersion recording chamber perfused with artificial cerebrospinal fluid (ACSF) containing (in mM): 126 NaCl, 4 KCl, 1 $MgCl_2$, 1 $CaCl_2$, 1 NaH_2PO_4, 26 $NaHCO_3$, 20 glucose, perfused with 95% O_2 and 5% CO_2. Flow of ACSF into the recording chamber was at a rate of 3 mL/min and its temperature was maintained at 33–34 °C by a temperature controller (TC-324C, Warner Instruments). An upright microscope (SliceScope Pro 2000, Scientifica) with a 40X water immersion objective lens (LUMPLFLN40XW, Olympus), 490 nm LED

illumination (pE-100, CoolLED), and a GFP filter set (49002, Chroma) was used. Images were acquired at 10 Hz (2 × 2 digital binning, 1024 × 1024 pixel resolution) with an sCMOS camera (Prime BSI, Teledyne Photometrics) using Micro-manager open-source software for 30 sec before and 150 sec after taltirelin application. EZcalcium open-source MATLAB toolbox[41] was used for motion correction and automated ROI (region of interest) detection. Round-shaped, soma-like ROIs were manually selected for extracting neuronal fluorescence signals. Fluorescence signal of each MEA slice was obtained by averaging changes in fluorescence (deltaF/F) of individual neurons (n=336 cells from 6 slices). The fluorescence signal of individual MEA slices were used to obtain the average fluorescence trace shown in Extended Data Fig. 9k.

In vivo recording of MEA responses upon photoactivation of COApm inputs

MEA responses to COApm inputs in conditional Trhr KO mice were tested by recording local field potentials (LFPs) in anesthetized mice. $Trhr^{fl/fl}$ mice were unilaterally injected with AAV_2-hSyn-ChR2-EYFP in COApm and AAV_1-hSyn-GFP or AAV_1-hSyn-Cre in the ipsilateral MEApv. Four weeks after the viral injections, mice were anesthetized using a mixture of ketamine (100 mg/kg, intraperitoneal injection) and xylazine (10 mg/kg, intraperitoneal injection) and placed in a stereotaxic frame. An homemade optrode, which consists of an optic fiber (200um) and two-channel tungsten electrodes (5MΩ, 300um projection from the optic fiber tip), were lowered to MEApv. LFPs were recorded starting at DV=−5.0 mm from the bregma, while the electrode was being lowered, to find the locus of the maximum response evoked by a single pulse of photoactivation (405nm laser, 2mW, 10-msec) of COApm inputs. Recordings were amplified, band-pass filtered between 10 and 300 Hz and digitized at 10KHz using a Digital Lynx 4SX system (Neuralynx). TTL event signals for photoactivation from a pulse generator were aligned to the recorded waveforms using the Neuralynx system. Light-evoked local field potentials were analyzed off-line using a (ADInstrument, NeuroExplorer5). Three waveforms evoked by photostimulations delivered at 1-min intervals were averaged to obtain the baseline-to-negative peak amplitude for individual animals.

RNA sequencing

Labeling of COApm cells projecting to MEA. Vglut2-Cre mice received stereotaxic injections of a virus mixture (AAV1-syn-FLEX-TTA and AAV1-TRE-B19G, total 0.5μl)[42] into MEApv (±2.1 ML, −1.7 AP, −5.6 DV). After 2 weeks, glycoprotein gene deleted rabies virus (RVΔG-4EGFP-L10a (EnvA)) was targeted to the same coordinates. Five days later, COApm tissues were harvested and immediately used for TRAP purifications as described below. For the control group, 100μl of AAV.PHP.eB-Syn-L10a-EGFP (1.13×1011 VG/mouse concentration; SignaGen Laboratories, Frederick, MD) was retro-orbitally injected. COApm tissue was harvested at 3-weeks post-injection and used immediately for TRAP purifications.

TRAP purifications. Brain tissue dissections were performed on ice after cooling the head in liquid nitrogen for 4 sec. After dissection, cell type-specific mRNAs were purified according to the established TRAP protocol[43]. COApm tissue was homogenized with a glass/Teflon power-driven Potter-Elvehjem homogenizer in an ice-cold lysis buffer

(150mM KCl, 10 mM HEPES [pH 7.4], 5mM MgCl2, 0.5mM dithiothreitol, 100 μg/mL cycloheximide, 20 U/μL SUPERaseIn RNase Inhibitor, 40 U/μL RNasin Plus Rnase Inhibitor, and EDTA-free protease inhibitors). Following homogenization, samples were centrifuged at 2,000 × g at 4°C for 10 min and the supernatant was transferred to a new tube. NP-40 (final concentration 1%) and 1,2-Diheptanoyl-sn-glycero-3-phosphocholine (DHPC, final concentration 15mM) were subsequently added and samples were incubated on ice for 5 min. Samples were centrifuged at 13,000 × g at 4°C for 10 min and the supernatant was transferred to a new tube. Streptavidin Dynabeads (ThermoFisher Scientific, Waltham MA) coated with biotin-linked mouse anti-GFP antibodies were then added to this supernatant and the samples were incubated overnight at 4°C with end-over-end rotation. Beads were collected on a magnetic rack and washed three times with wash buffer (350mM KCl, 10mM HEPES [pH 7.4], 5mM MgCl2, 0.5mM dithiothreitol, 100μg/mL cycloheximide, 1% NP-40). RNA was subsequently purified using the Absolutely RNA Isolation Nanoprep kit (Agilent Technologies, Santa Clara CA). To ensure quality and accurate quantitation, purified RNA was run on a Bioanalyzer using the RNA 6000 Pico Kit (Agilent Technologies, Santa Clara CA).

TRAP RNA sequencing and analysis. Purified TRAP samples were prepared for RNA-Seq using the Takara Bio Smart-Seq v4 kit (Takara Bio USA, Inc.). RNA-Seq was performed on an Illumina HiSeq 4000 at the University of California, San Francisco Functional Genomics Core. FASTQ files were aligned to the Mus musculus genome build GRCm38 and annotation build 96 (reference FASTA and GTF file) using STAR v2.7.2b. Read counts were generated by STAR using the --quantMode GeneCounts option, using the default options. Only mapped reads uniquely assigned to the mouse genome were used for differential expression testing. These were imported into R and then converted to normalized read counts with DESeq2[44]. Differential Expression was performed using DESeq2, and significant genes were filtered by a q-value (False Discovery Rate) threshold of 1e-15. To remove systemic bias possible from the use of rabies virus[45,46], genes involved in the following MSigDB hallmark gene sets were further removed: Interferon Gamma Response, Interferon Alpha Response, Allograft Rejection, IL6 JAK STAT3 Signaling, TNFa Signaling via NF-kB, Inflammatory Response, Complement, G2M Checkpoint, E2F Targets, and IL2 STAT5 Signaling. These differentially expressed genes were then compared to the set of COApm-enriched genes [relative to the grey matter] obtained from Allen Brain Atlas Differential Search with the expression threshold set to 1. For KEGG pathway analysis, differentially expressed genes were processed using Enrichr[47,48].

Statistics and reproducibility

Statistical analyses were performed using GraphPad Prism. Sample sizes were chosen on the basis of similar previous studies[20,49], and not on statistical methods to predetermine sample sizes. Within each iteration of an experiment, mice were randomly assigned to groups with approximately balanced sample size. Behavioral results from mice with inaccurate targeting of viral infection or cannula implantations were excluded.

Extended Data

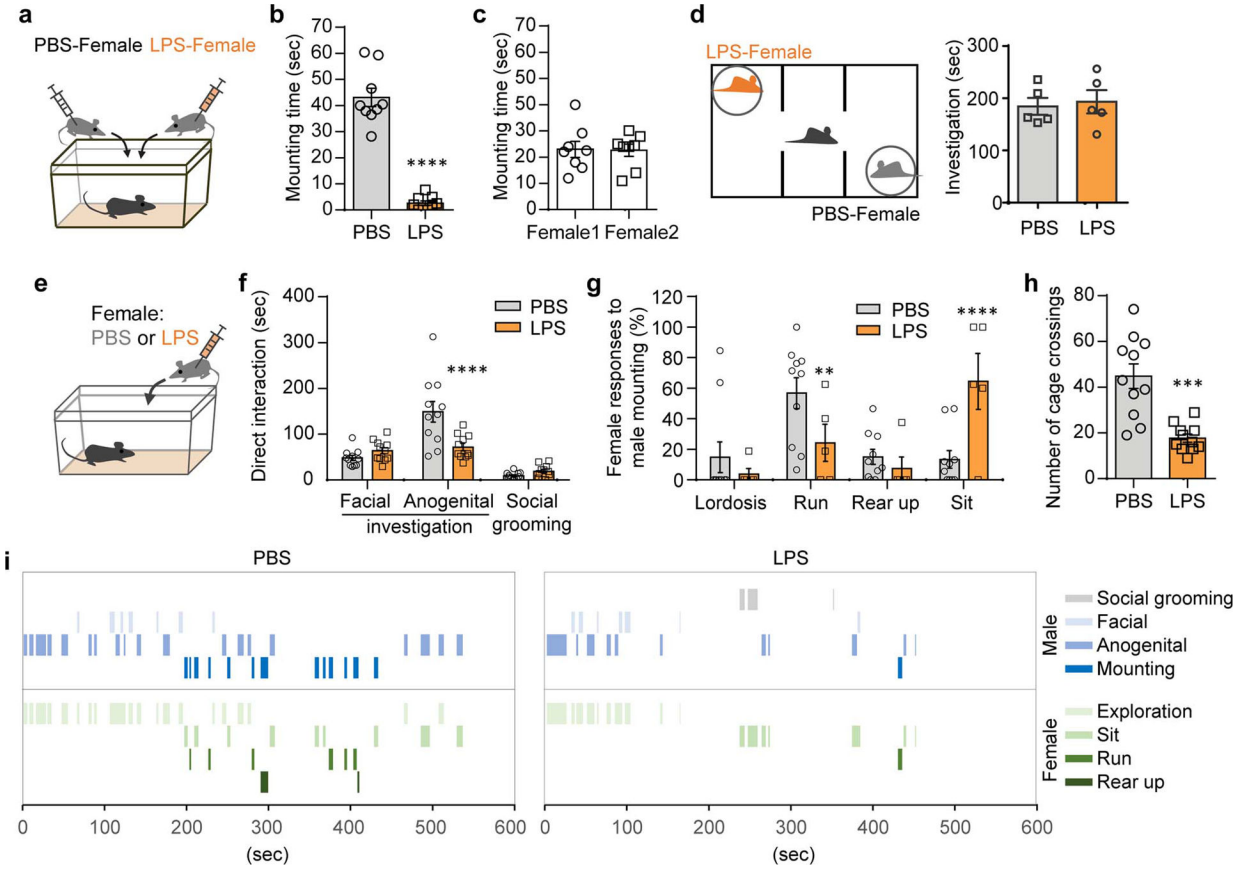

Extended Data Figure 1. Male mice avoid mounting sick females.

a,b, Male mice were presented with a pair of estrus females each injected intraperitoneally with either PBS (PBS-female) or LPS (LPS-female) (**a**). Mounting time during a 10-min test (**b**) (n=9; from 2 independent experiments). **c,** Mounting time for male mice presented with two untreated, healthy females (n=8; from 2 independent experiments). **d,** Investigation time of PBS- and LPS-females during a 10-min three-chamber assay (n=5; from 2 independent experiments). **e-i,** These data are associated with Fig.1a–e. Duration of other typical male behaviors while engaged in direct interactions with a PBS- or LPS- female (**e,f**). Percentage of individual female behaviors during males' mounting attempts (**g**) and the number of cage crossings (**h**). Representative traces of male and female behaviors during direct interactions (**i**). ** P<0.01, *** P<0.001 and **** P<0.0001 calculated by paired two-tailed t-test (**b),** two-way ANOVA with Sidak's post-hoc test (**f,g)** and unpaired two-tailed t-test (**h**). Graphs indicate mean ± s.e.m. p-values are described in the supplementary statistical information file.

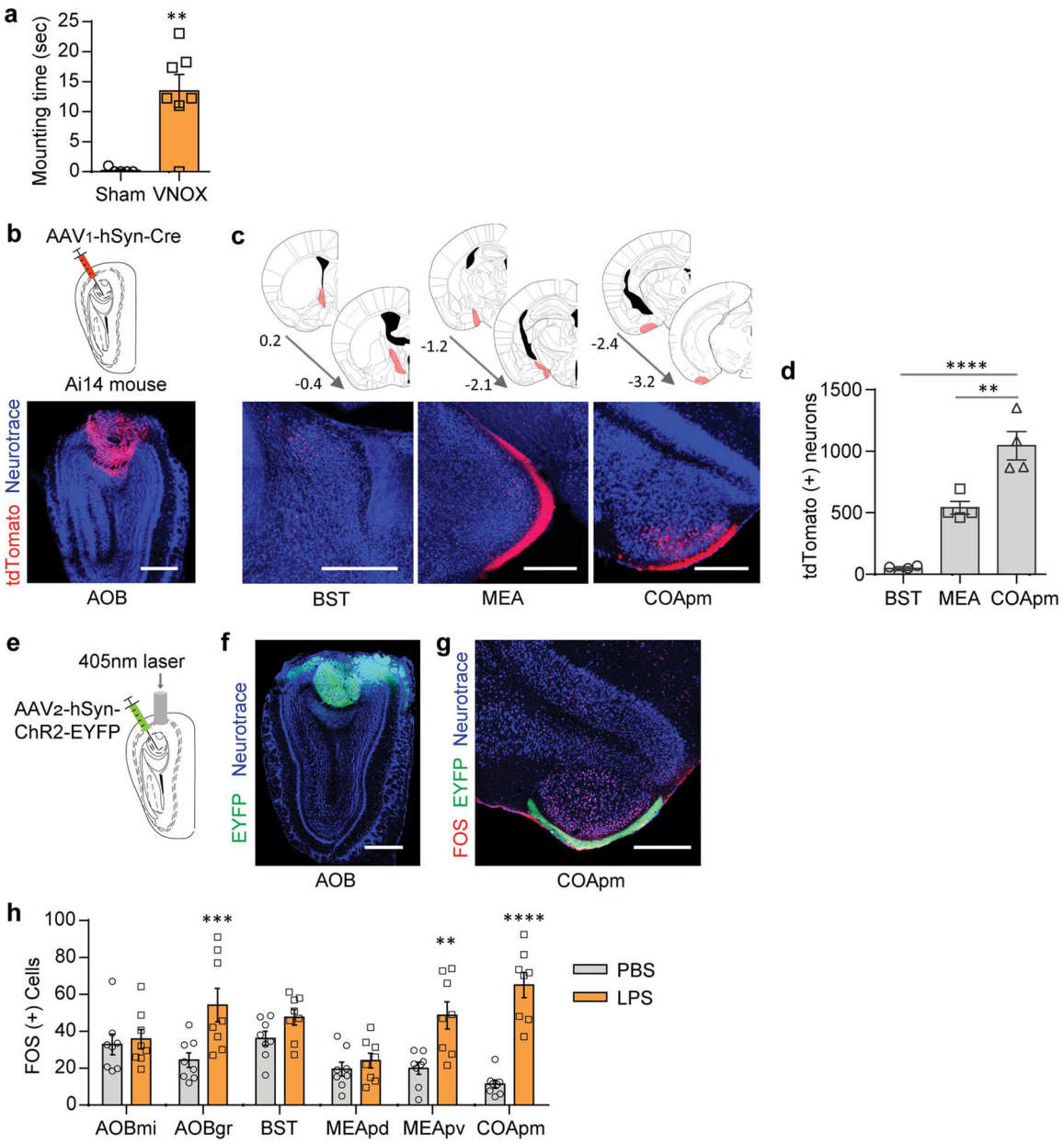

Extended Data Figure 2. Role of the vomeronasal pathway in mounting behavior.

a, Mounting time for males with a sham surgery (Sham) or the VNO removed (VNOX) towards LPS-females (Sham, n=5 and VNOX, n=7; from 2 independent experiments). **b-d,** Virus encoding the anterograde trans-synaptic tracer (AAV_1-hSyn-Cre) was targeted to the accessory olfactory bulb (AOB) in Ai14 reporter mice that express tdTomato in a Cre-dependent manner (**b**). Representative images (**c**) and quantification (**d**) of trans-synaptically labeled tdTomato(+) neurons in BST, MEA, and COApm at the specified anterior-posterior axis (n=4; from 3 independent experiments). Scale bar=500μm. **e-g,** Virus encoding ChR2 (AAV_2-hSyn-hChR2-EYFP) was targeted to the AOB (**e,f**). Representative image of FOS expression in the COApm upon photoactivation of the AOB, from n=3 animals (**g**). Scale bar=500μm. **h,** These data are associated with Fig.1g. Number of FOS-

expressing neurons in the vomeronasal pathway after interaction with PBS- or LPS-females. ** P<0.01, *** P<0.001 and **** P<0.0001 calculated by unpaired two-tailed t-test (**a**), one-way ANOVA with Bonferroni's post-hoc test (**d**) and two-way ANOVA with Sidak's post-hoc test (**h**). Graph indicates mean ± s.e.m. p-values are described in the supplementary statistical information file.

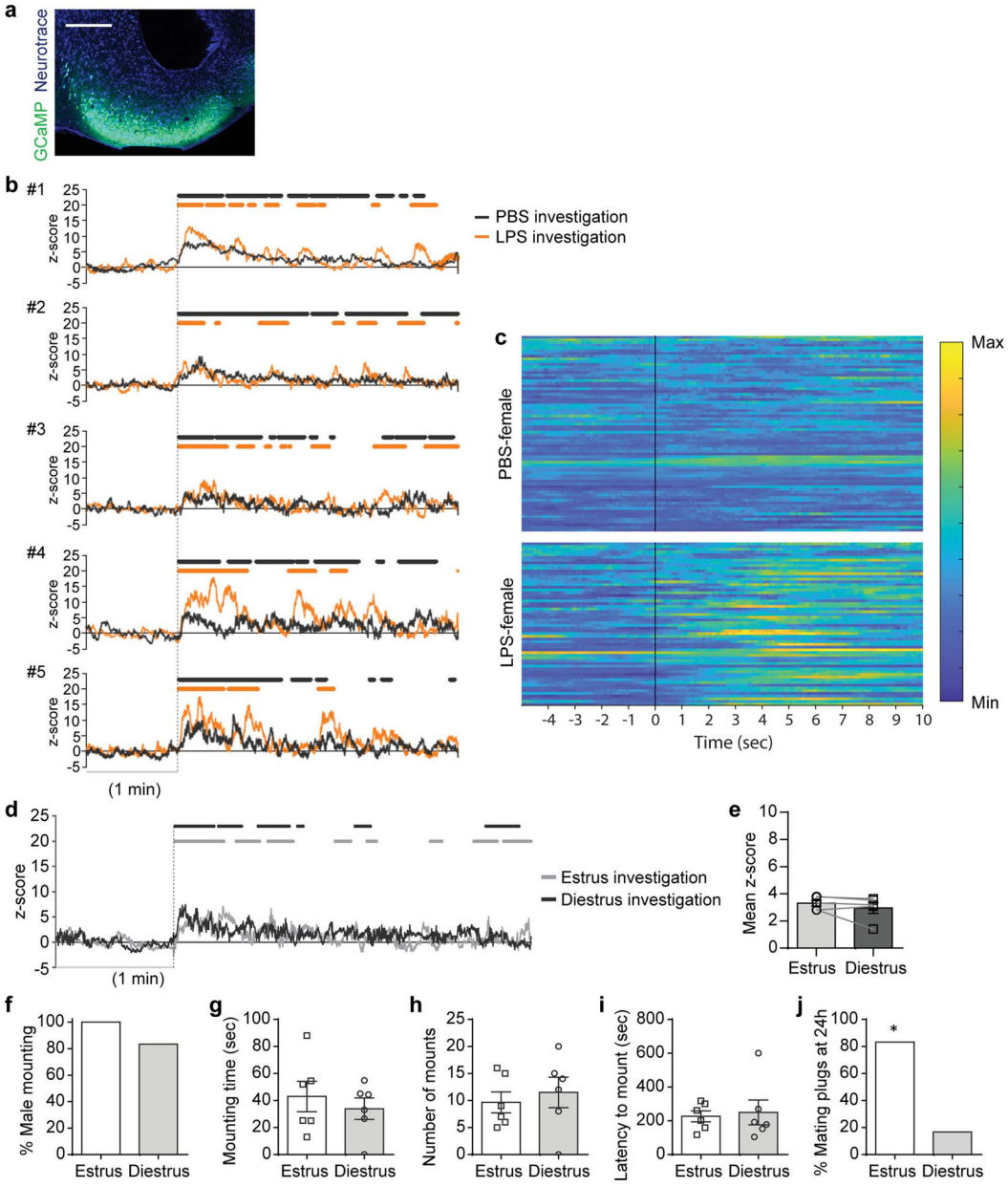

Extended Data Figure 3. Investigation of LPS-females induces neural activity in the COApm of males.

a-c, These data are associated with Fig.1h–o. Representative image of GCaMP6s expression in the COApm (**a**). Individual traces of COApm bulk fluorescence signal during interactions with a PBS- or LPS-female (**b**). Heatmap of normalized COApm responses to PBS- or LPS-females. Each row represents a single investigation event. Investigation events were

pooled from 6 animals from 3 independent experiments. Time=0 indicates initiation of investigation (**c**). Scale bar=300μm. **d,e,** Virus encoding GCaMP6s (AAV_1-Syn-GCaMP6s) was targeted to the COApm for fiber photometry recordings. Male mice were sequentially presented with an estrus or diestrus female in counterbalanced sessions. Representative traces of COApm bulk fluorescence signal (**d**) and the mean z-score of the fluorescence during direct investigation of the estrus or diestrus female (**e**) (Estrus, n=5 and Diestrus, n=5; from 3 independent experiments). **f-j,** Male mounting behaviors towards an estrus or diestrus, healthy female. Percent male mounting (**f**), mounting time (**g**), number of mounts (**h**), latency to mount (**i**), and percent female partners with mating plugs (**j**) (Estrus, n=6 and Diestrus, n=6; from 2 independent experiments). *P<0.05 calculated by Chi-Square Test of Independence (**j**). Graph indicates mean ± s.e.m. p-values are described in the supplementary statistical information file.

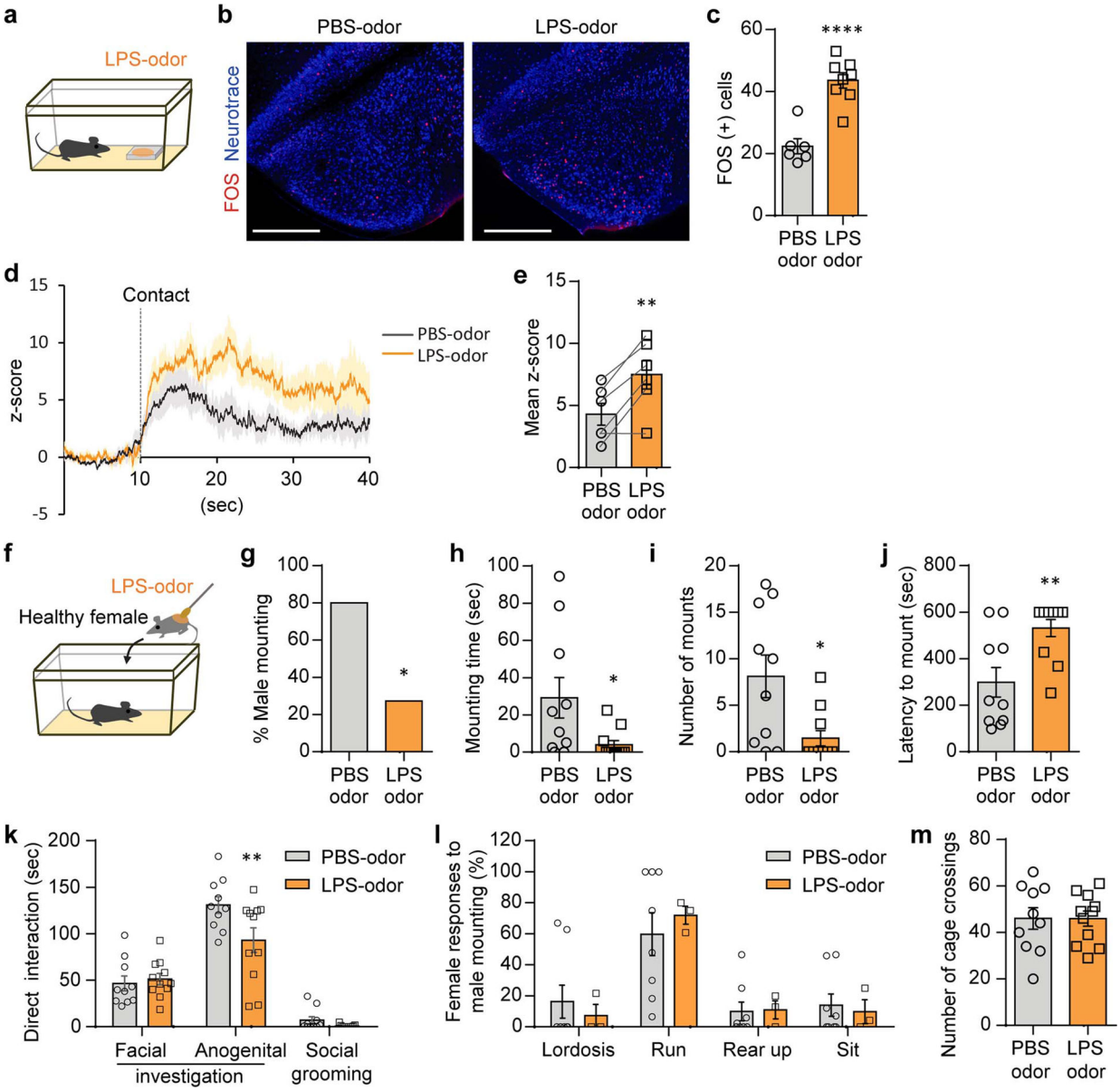

Extended Data Figure 4. LPS-odor suppresses male mating behaviors.

a-c, Male mice were presented with PBS- or LPS-odor (**a**). Representative images (**b**) and quantification (**c**) of FOS expression in the COApm of males after exposure to PBS- or LPS-odor (PBS-odor, n=6 and LPS-odor, n=8; from 2 independent experiments). Scale bar=500μm. **d,e,** Virus encoding GCaMP6s (AAV_1-Syn-GCaMP6s) was targeted to the COApm for fiber photometry recordings. Male mice were sequentially presented with a PBS- or LPS-odor in counterbalanced sessions. Traces of COApm bulk fluorescence signal (solid line=average, shaded area=s.e.m.) (**d**) and the mean z-score of the fluorescence during the first 20 sec of direct investigation of the odor (**e**) (n=6; from 3 independent experiments). **f-m,** Male mice were presented with a healthy female painted with PBS- or LPS-odor (**f**). Percent male mounting (**g**), mounting time (**h**), number of mounts (**i**), latency to mount (**j**), and duration of additional male behaviors while engaged in direct interactions with

the female (**k**). Percentage of female behaviors in response to males' mounting attempts (**l**) and the number of cage crossings (**m**) (PBS-odor, n=10 and LPS-odor, n=11; from 2 independent experiments). *P<0.05, **P<0.01 and ****P<0.0001 calculated by unpaired two-tailed t-test (**c**,**h-j**), paired two-tailed t-test (**e**), Chi-Square Test of Independence (**g**) and two-way ANOVA with Sidak's post-hoc test (**k**). Graphs indicate mean ± s.e.m. p-values are described in the supplementary statistical information file.

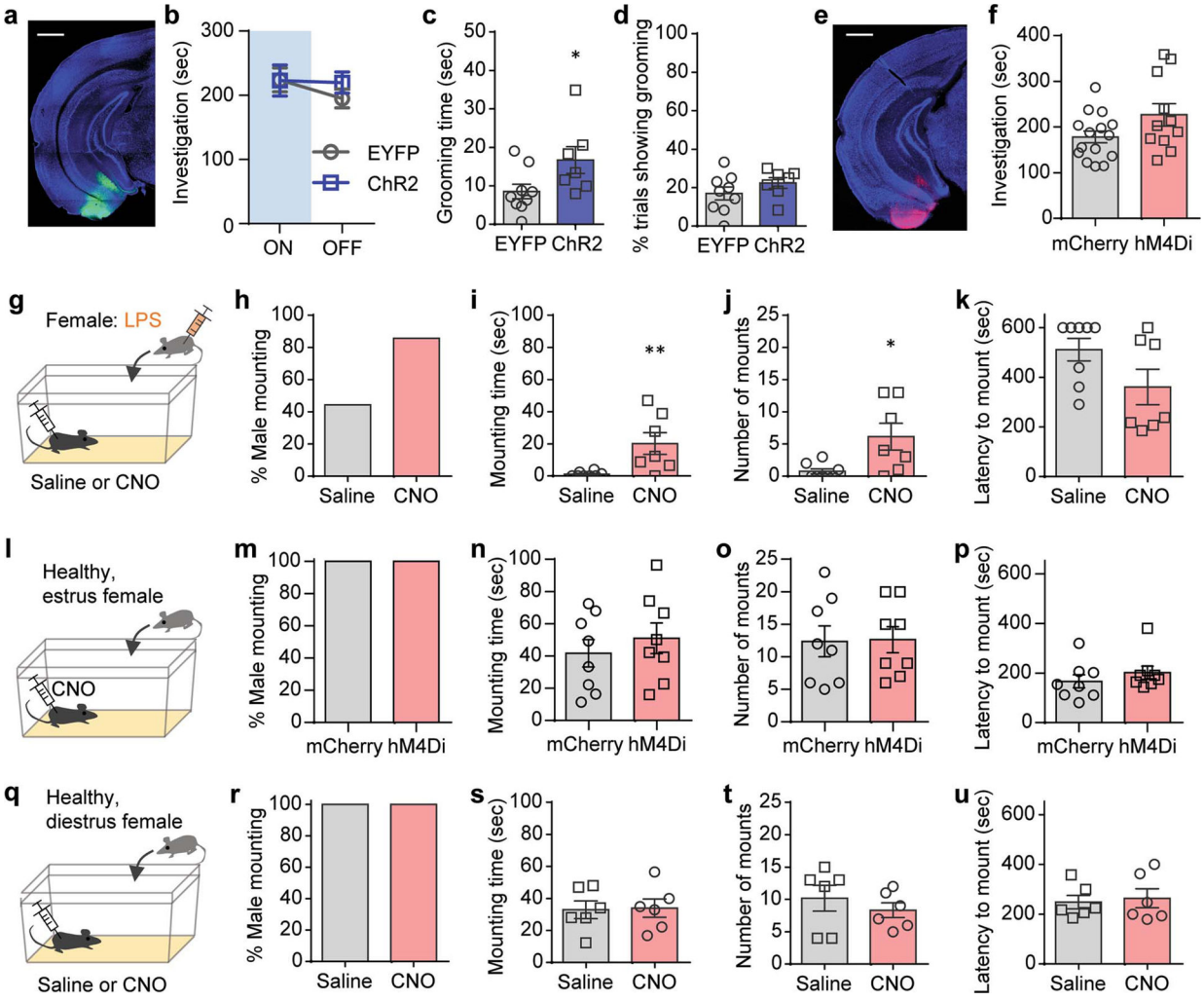

Extended Data Figure 5. COApm mediates suppression of mating behaviors towards unhealthy females.

a-d, These data are associated with Fig.2a–e. Representative image of ChR2 expression in the COApm (**a**). Total direct investigation time of healthy females in the presence (ON) and absence (OFF) of COApm photoactivation (**b**). Duration of self grooming (**c**) and percentage of photoactivation trials with self grooming (**d**). Scale bar=1mm. **e,f,** These data are associated with Fig.2i–m. Representative image of hM4Di expression in the COApm (**e**) and total direct investigation time of LPS-females (**f**). Scale bar=1mm. **g-k,** Additional control experiments for data in Fig.2i–m. Male mice expressing inhibitory DREADD (hM4Di, AAV_2-hSyn-hM4D(Gi)-mCherry) in COApm were injected with either saline or CNO

and tested for mounting behavior towards LPS-females (**g**). Percent male mounting (**h**), mounting time (**i**), number of mounts (**j**), and latency to mount (**k**) (Saline, n=8 and CNO, n=7; from 2 independent experiments). **l-p,** Male mice expressing mCherry (AAV_2-hSyn-mCherry) or inhibitory DREADD (hM4Di, AAV_2-hSyn-hM4D(Gi)-mCherry) in COApm were injected with CNO and tested for mounting behavior towards untreated, healthy estrus females (**l**). Percent male mounting (**m**), mounting time (**n**), number of mounts (**o**), and latency to mount (**p**) (mCherry, n=8 and hM4Di, n=8; from 2 independent experiments). **q-u,** Male mice expressing inhibitory DREADD (hM4Di, AAV_2-hSyn-hM4D(Gi)-mCherry) in COApm were injected with saline or CNO and tested for mounting behavior toward untreated, healthy diestrus females (**q**). Percent male mounting (**r**), mounting time (**s**), number of mounts (**t**), and latency to mount (**u**) (Saline, n=6 and CNO, n=6; from 2 independent experiments). *P<0.05, **P<0.01 calculated by unpaired two-tailed t-test (**c**,**i**,**j**). Graphs indicate mean ± s.e.m. p-values are described in the supplementary statistical information file.

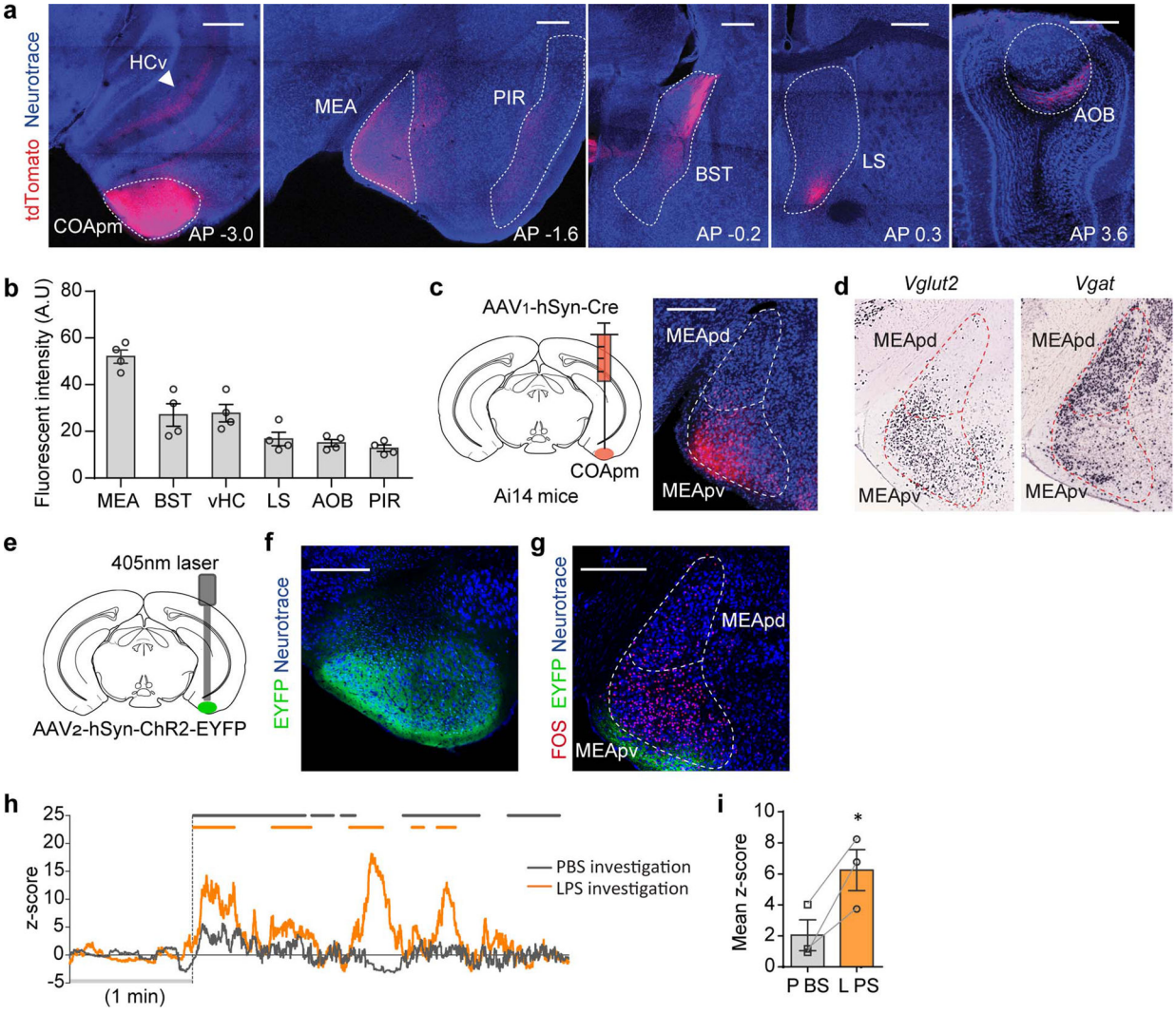

Extended Data Figure 6. COApm neurons preferentially project to MEA-Vglut2(+) neurons.

a-b, Virus encoding the anterograde tracer (AAV_2-hSyn-tdTomato) was targeted to the COApm. Total fluorescence intensity was measured in sub-regions receiving COApm axonal projections: MEA, BST, ventral hippocampus (HCv), lateral septum (LS), AOB and piriform cortex (PIR) (n=4 mice; from 2 independent experiments). Scale bar=500μm. **c**, Virus encoding the anterograde trans-synaptic tracer (AAV_1-hSyn-Cre) was targeted to the COApm of Ai14 reporter mice that express tdTomato in a Cre-dependent manner. Representative image of MEA post-synaptic neurons at anterior-posterior (AP) −1.7 mm, from 3 independent experiments. Scale bar=300μm. **d,** mRNA expression of *Vglut2* and *Vgat* in MEA (Image credit: Allen Institute). **e-g,** ChR2 (AAV_2-hSyn-ChR2-EYFP) was targeted to the COApm (**e**). Representative images of ChR2 expression in COApm (**f**) and FOS expression in MEA upon photoactivation of COApm (**g**) (n=3; from 2 independent experiments). Scale bar=300μm. **h,i,** Virus encoding GCaMP6s (AAV_1-Syn-GCaMP6s) was targeted to the MEA of Vglut2-Cre mice for fiber photometry recordings. Male mice were sequentially presented with a PBS- or LPS-female in counterbalanced sessions. Representative traces of MEA-vGlut2(+) bulk fluorescence signal (**h**) and the mean z-score of the fluorescence during direct investigation of the PBS- or LPS-female (**i**) (n=3; from 2 independent experiments). *P<0.05 calculated by paired two-tailed t-test (**i**). Graphs indicate mean ± s.e.m. p-values are described in the supplementary statistical information file.

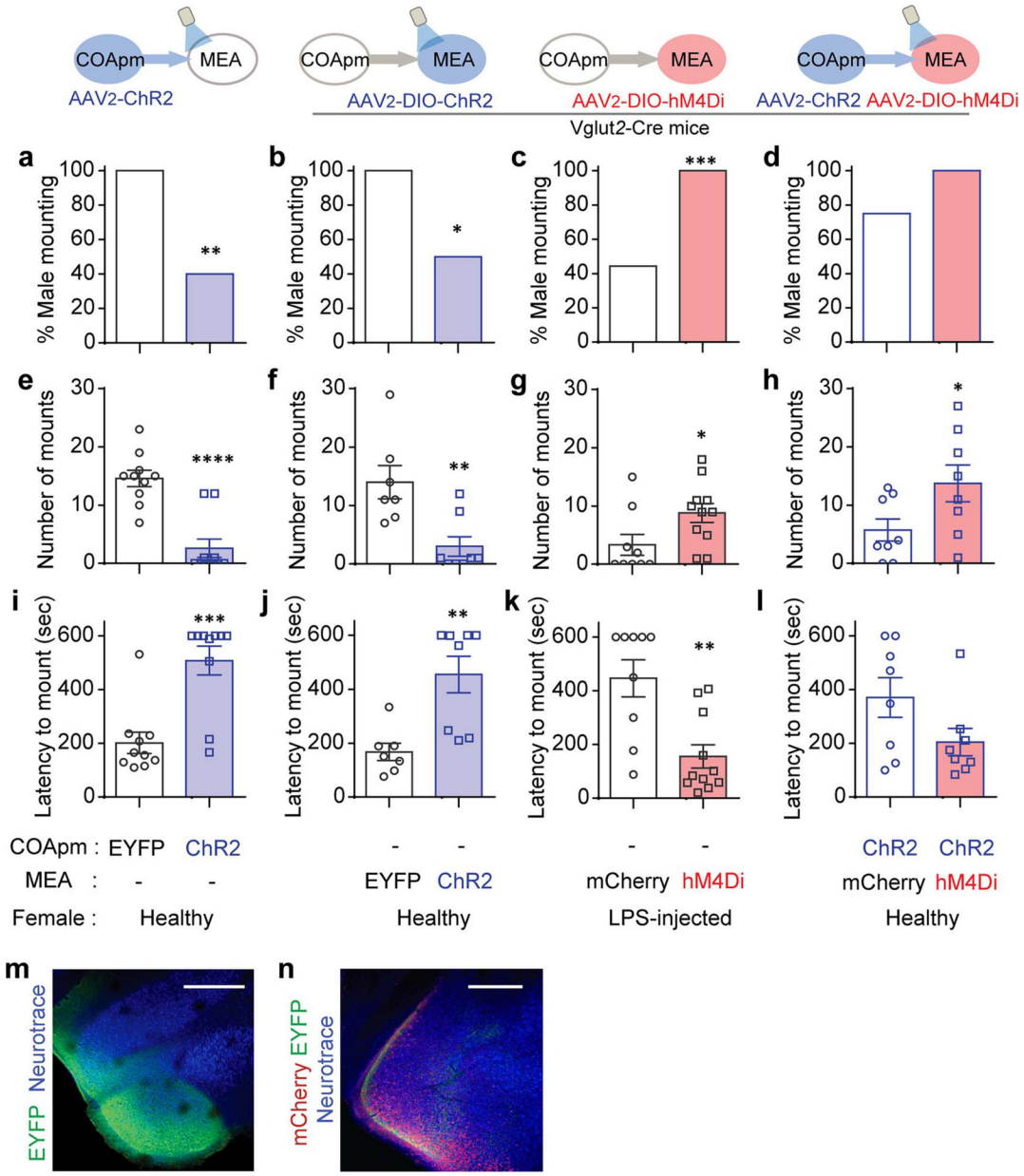

Extended Data Figure 7. COApm suppresses male mating behaviors by engaging MEA-Vglut2(+) neurons.

These data are associated with Fig.3f–i. Percent male mounting (**a-d**), number of mounts (**e-h**), latency to mount (**i-l**). Representative images of ChR2 expression in COApm (**m**) and hM4Di expression in MEA (**n**) of Vglut2-Cre mice with concurrent photoactivation of COApm-MEA projections and hM4Di-inhibition of MEA-Vglut2(+) neurons. Scale bar=500μm. **P*<0.05, ***P*<0.01, ****P*<0.001 and *****P*<0.0001 calculated by Chi-Square Test of Independence (**a-c**) and unpaired two-tailed *t*-test (**e-k**). Graphs indicate mean ± s.e.m. p-values are described in the supplementary statistical information file.

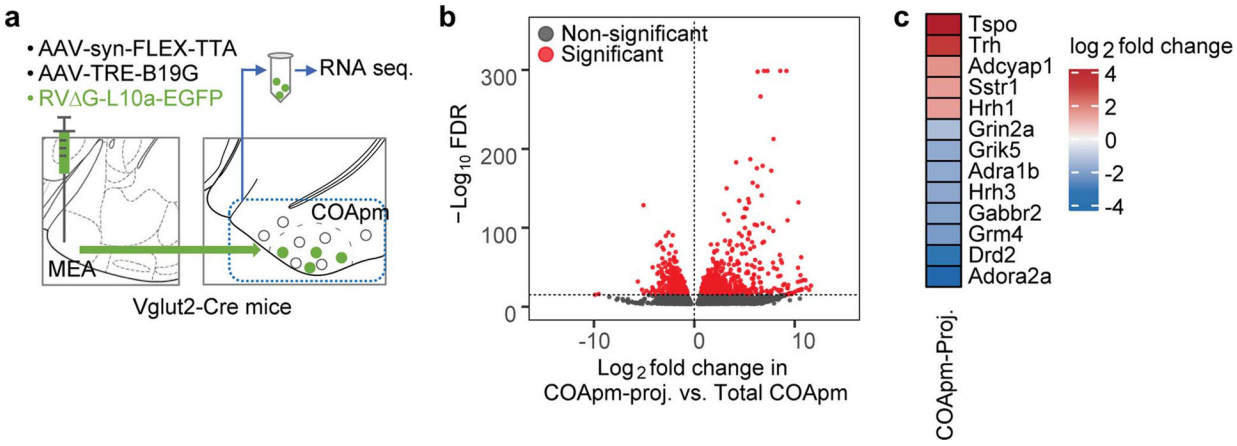

Extended Data Figure 8. Summary of gene expression profiling in COApm neurons projecting to MEA-Vglut2(+) neurons.

a, A combination of AAV_1-syn-FLEX-TTA and AAV-TRE-B19G, and RVΔG-L10a-EGFP were sequentially injected into the MEA of Vglut2-Cre mice to label COApm neurons projecting to MEA-Vglut2(+) neurons (COApm-proj). COApm tissue was harvested and immediately used for TRAP analyses. Control mice were injected with AAV.PHP.eB-Syn-L10a-EGFP via retro-orbital injection in order to label COApm neurons with L10a-EGFP independently of their efferent projections (Total COApm). **b,** Volcano plot showing $\log_2$-fold change plotted against $-\log_{10}$ FDR for the labeled COApm neurons projecting to the MEA-Vglut2(+) population (COApm-Proj.) compared to the Total COApm. Differentially expressed genes that pass the threshold for the FDR are highlighted in red. **c,** Heatmap showing COApm-differentially expressed genes that belong to the KEGG neuroactive ligand-receptor interaction pathway. p-values are described in the supplementary statistical information file.

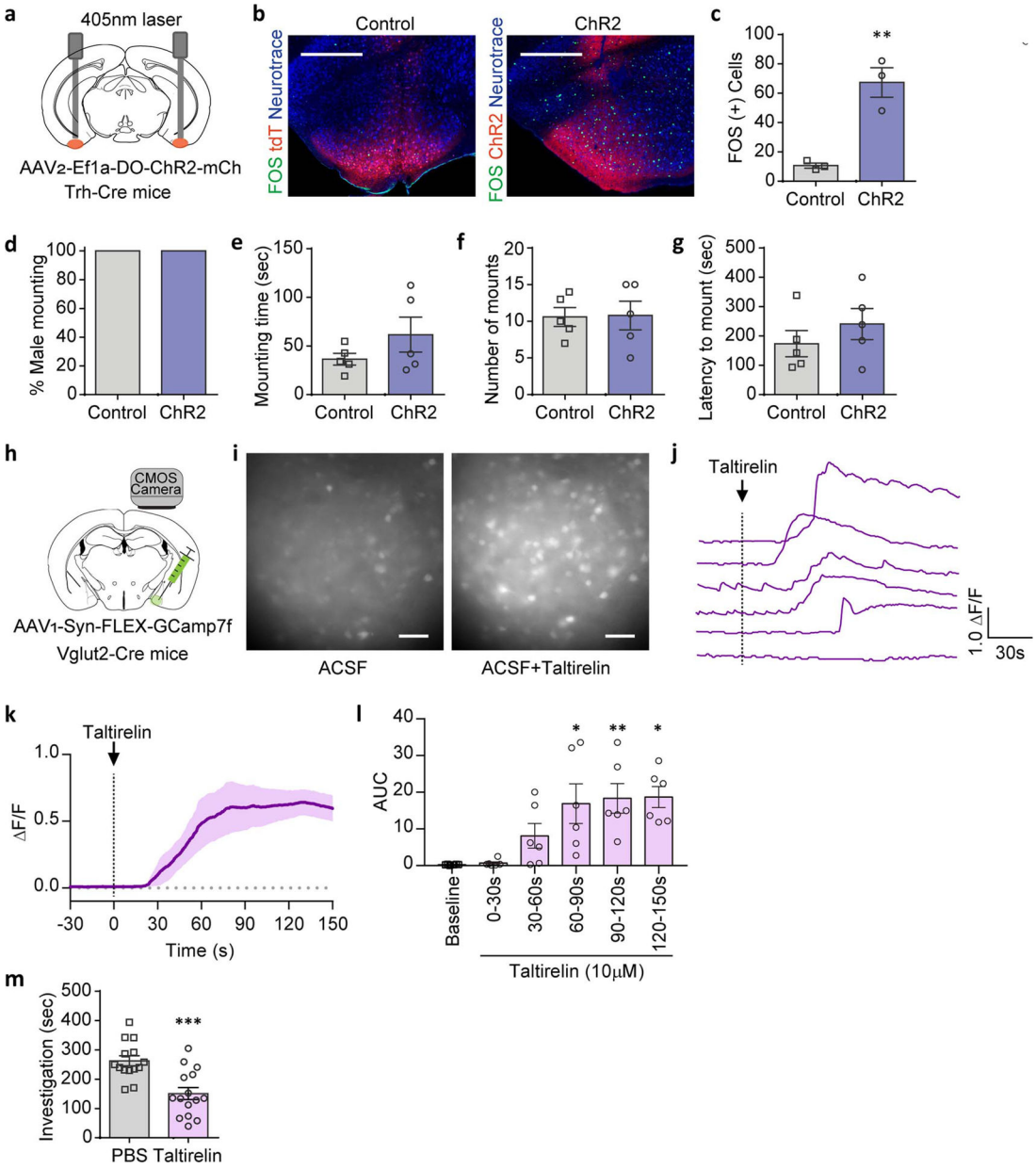

Extended Data Figure 9. COApm-TRH(+) neurons mediate the suppression of male mating towards unhealthy females.

a-g, Trh-Cre male mice expressing tdTomato ($AAV_{1/2}$-Ef1a-DO-DIO-tdTomato(tdT)-EGFP, Control) or ChR2 ($AAV_{1/2}$-Ef1a-DO-ChR2-mCherry, ChR2) in Cre(−) neurons were tested for mating behaviors towards healthy females with COApm photoactivation (**a**). Representative images (**b**) and quantification (**c**) of FOS expression in COApm. Percent male mounting (**d**), mounting time (**e**), number of mounts (**f**), and latency to mount (**g**) with photoactivation of COApm-TRH(−) cells (Control, n=5 and ChR2, n=5; from 2 independent experiments). Scale bar=500μm. **h-l,** Calcium imaging of MEA brain slices from Vglut2-Cre mice expressing GCaMP7f (AAV_1-hSyn-FLEX-GCaMP7f) in MEA-Vglut2(+) neurons upon taltirelin (10 μM) application (**h**). Representative images of MEA slices before (−15s)

and after (+35s) taltirelin application (**i**). Example traces of fluorescence signal from individual neurons (**j**) and the average of the fluorescence signal (solid line=average, shaded area=s.e.m.) (**k**) upon taltirelin application. Area under the curve (AUC) of the average fluorescence signal from individual MEA slices binned every 30 sec (**l**) (n=6 slices, from 3 mice). Scale=50μm. **m,** These data are associated with Fig.4k–o. Total duration of direct investigation following microinjection of the TRH analog taltirelin into MEA. *P<0.05, **P<0.01 and ***P<0.001 calculated by unpaired two-tailed t-test (**c,m**) and Friedman test with Dunn's multiple comparisons test (**l**). Graphs indicate mean ± s.e.m. p-values are described in the supplementary statistical information file.

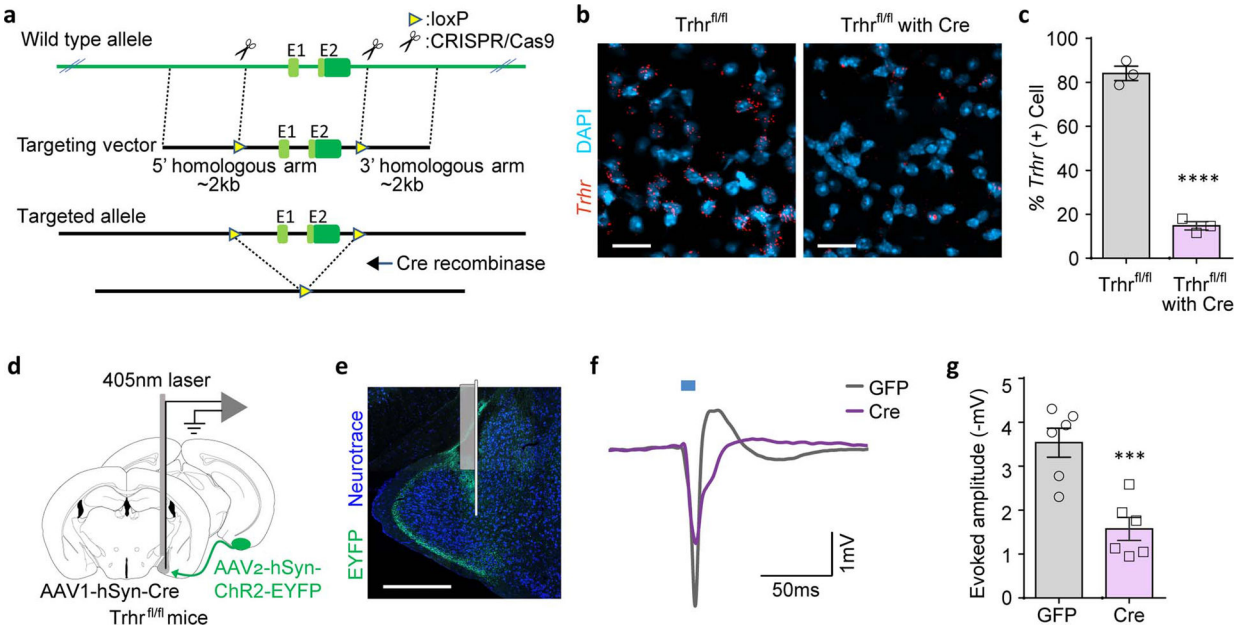

Extended Data Figure 10. Suppression of mating engages TRH-TRHR signaling in the COApm-MEA projection.

a, Schematic depicting the targeting construct used to generate the Trhr conditional knock-out mouse line. **b,c** Representative images (AP −1.8 mm) (**b**) and quantification (**c**) of *Trhr* mRNA expression in the MEApv of Trhr$^{fl/fl}$ mice with or without Cre expression (AAV_1-hSyn-Cre) (Trhr$^{fl/fl}$, n=3 and Trhr$^{fl/fl}$ with Cre, n=3; from 2 independent experiments). Scale bar=20μm. **d-g,** In vivo recordings of MEA responses to COApm inputs in Trhr conditional knock-out mice. Trhr$^{fl/fl}$ mice were injected with AAV_2-hSyn-ChR2-EYFP in COApm and either AAV_1-hSyn-GFP (GFP) or AAV_1-hSyn-Cre (Cre) in MEApv. Local field potentials evoked by a 10-msec photoactivation were recorded from MEApv in anesthetized mice using an optrode (**d**). Representative image of electrode localization (**e**). Representative waveforms (**f**) and amplitudes (baseline-to-negative peak) of MEApv responses evoked by photoactivation of COApm inputs (**g**) (GFP, n=6 and Cre, n=6; from 6 independent experiments). Scale bar=300μm. ***P<0.001 and ****P<0.0001 calculated by unpaired two-tailed t-test (**c,g**). Graphs indicate mean ± s.e.m. p-values are described in the supplementary statistical information file.

Supplementary Material

Refer to Web version on PubMed Central for supplementary material.

Acknowledgements

We thank N. Soares, M. Andina, K. Ronayne and I.D. Mejia for assistance with experiments and B. Noro and M. Trombly for critical reading of the manuscript. We thank J. Huh for his contribution to the conceptual development of the project. We thank B. Lowell for generously sharing the *Trh*-Cre mouse line. We thank H. Choi for the fiber photometry set-up. This work was supported by the National Institute of Mental Health grants R01 MH122270 and R01 MH106497 (G.B.C.), the JPB Foundation (M.H. and G.B.C), Simons Center for the Social Brain Postdoctoral Fellowship (J.K. and H.K.C) and the Picower Fellows (J.K. and H.L.).

Data availability

Source data are provided in the supplementary information. Sequencing datasets are publicly available in NCBI GEO under accession # GSE167176. All data are available from the corresponding author upon request.

References

1. Tinbergen N The study of instinct. New York, NY: Claredon Press/Oxford University Press (1951).
2. Altizer S et al. Social Organization and Parasite Risk in Mammals: Integrating Theory and Empirical Studies. Annual Review of Ecology, Evolution, and Systematics 34, 517–547 (2003).
3. Hart BL Behavioral adaptations to pathogens and parasites: five strategies. Neuroscience and biobehavioral reviews 14, 273–294, doi:10.1016/s0149-7634(05)80038-7 (1990). [PubMed: 2234607]
4. Ehman KD & Scott ME Female mice mate preferentially with non-parasitized males. Parasitology 125, 461–466, doi:10.1017/s003118200200224x (2002). [PubMed: 12458830]
5. Chen P & Hong W Neural Circuit Mechanisms of Social Behavior. Neuron 98, 16–30, doi:10.1016/j.neuron.2018.02.026 (2018). [PubMed: 29621486]
6. Chamero P et al. Identification of protein pheromones that promote aggressive behaviour. Nature 450, 899–902, doi:10.1038/nature05997 (2007). [PubMed: 18064011]
7. Hashikawa K, Hashikawa Y, Falkner A & Lin D The neural circuits of mating and fighting in male mice. Current opinion in neurobiology 38, 27–37, doi:10.1016/j.conb.2016.01.006 (2016). [PubMed: 26849838]
8. Stowers L, Holy TE, Meister M, Dulac C & Koentges G Loss of sex discrimination and male-male aggression in mice deficient for TRP2. Science 295, 1493–1500, doi:10.1126/science.1069259 (2002). [PubMed: 11823606]
9. Leypold BG et al. Altered sexual and social behaviors in trp2 mutant mice. Proceedings of the National Academy of Sciences of the United States of America 99, 6376–6381, doi:10.1073/pnas.082127599 (2002). [PubMed: 11972034]
10. Medzhitov R Toll-like receptors and innate immunity. Nature reviews. Immunology 1, 135–145, doi:10.1038/35100529 (2001).
11. Boillat M et al. The vomeronasal system mediates sick conspecific avoidance. Current biology : CB 25, 251–255, doi:10.1016/j.cub.2014.11.061 (2015). [PubMed: 25578906]
12. Riviere S, Challet L, Fluegge D, Spehr M & Rodriguez I Formyl peptide receptor-like proteins are a novel family of vomeronasal chemosensors. Nature 459, 574–577, doi:10.1038/nature08029 (2009). [PubMed: 19387439]
13. Liberles SD et al. Formyl peptide receptors are candidate chemosensory receptors in the vomeronasal organ. Proceedings of the National Academy of Sciences of the United States of America 106, 9842–9847, doi:10.1073/pnas.0904464106 (2009). [PubMed: 19497865]

14. Kavaliers M, Choleris E, Agmo A & Pfaff DW Olfactory-mediated parasite recognition and avoidance: linking genes to behavior. Hormones and behavior 46, 272–283, doi:10.1016/j.yhbeh.2004.03.005 (2004). [PubMed: 15325228]
15. Scalia F & Winans SS The differential projections of the olfactory bulb and accessory olfactory bulb in mammals. The Journal of comparative neurology 161, 31–55, doi:10.1002/cne.901610105 (1975). [PubMed: 1133226]
16. Boehm U The vomeronasal system in mice: from the nose to the hypothalamus- and back! Seminars in cell & developmental biology 17, 471–479, doi:10.1016/j.semcdb.2006.04.013 (2006). [PubMed: 16765613]
17. Choi GB et al. Lhx6 delineates a pathway mediating innate reproductive behaviors from the amygdala to the hypothalamus. Neuron 46, 647–660, doi:10.1016/j.neuron.2005.04.011 (2005). [PubMed: 15944132]
18. Li Y et al. Neuronal Representation of Social Information in the Medial Amygdala of Awake Behaving Mice. Cell 171, 1176–1190 e1117, doi:10.1016/j.cell.2017.10.015 (2017). [PubMed: 29107332]
19. Ishii KK et al. A Labeled-Line Neural Circuit for Pheromone-Mediated Sexual Behaviors in Mice. Neuron 95, 123–137 e128, doi:10.1016/j.neuron.2017.05.038 (2017). [PubMed: 28648498]
20. Hong W, Kim DW & Anderson DJ Antagonistic control of social versus repetitive self-grooming behaviors by separable amygdala neuronal subsets. Cell 158, 1348–1361, doi:10.1016/j.cell.2014.07.049 (2014). [PubMed: 25215491]
21. Wickersham IR, Finke S, Conzelmann KK & Callaway EM Retrograde neuronal tracing with a deletion-mutant rabies virus. Nature methods 4, 47–49, doi:10.1038/nmeth999 (2007). [PubMed: 17179932]
22. Heiman M et al. A translational profiling approach for the molecular characterization of CNS cell types. Cell 135, 738–748, doi:10.1016/j.cell.2008.10.028 (2008). [PubMed: 19013281]
23. Suzuki M, Sugano H, Matsumoto K, Yamamura M & Ishida R Synthesis and central nervous system actions of thyrotropin-releasing hormone analogues containing a dihydroorotic acid moiety. Journal of medicinal chemistry 33, 2130–2137, doi:10.1021/jm00170a014 (1990). [PubMed: 2115588]
24. Hart BL Biological basis of the behavior of sick animals. Neuroscience and biobehavioral reviews 12, 123–137, doi:10.1016/s0149-7634(88)80004-6 (1988). [PubMed: 3050629]
25. Lopes PC, Block P & Konig B Infection-induced behavioural changes reduce connectivity and the potential for disease spread in wild mice contact networks. Scientific reports 6, 31790, doi:10.1038/srep31790 (2016). [PubMed: 27548906]
26. Van Kerckhove K, Hens N, Edmunds WJ & Eames KT The impact of illness on social networks: implications for transmission and control of influenza. American journal of epidemiology 178, 1655–1662, doi:10.1093/aje/kwt196 (2013). [PubMed: 24100954]
27. Stockmaier S, Bolnick DI, Page RA & Carter GG Sickness effects on social interactions depend on the type of behaviour and relationship. The Journal of animal ecology, doi:10.1111/1365-2656.13193 (2020).
28. Fischer S & Ehlert U Hypothalamic-pituitary-thyroid (HPT) axis functioning in anxiety disorders. A systematic review. Depression and anxiety 35, 98–110, doi:10.1002/da.22692 (2018). [PubMed: 29064607]
29. Baumgartner A Thyroxine and the treatment of affective disorders: an overview of the results of basic and clinical research. The international journal of neuropsychopharmacology 3, 149–165, doi:10.1017/S1461145700001887 (2000). [PubMed: 11343592]
30. Krashes MJ et al. An excitatory paraventricular nucleus to AgRP neuron circuit that drives hunger. Nature 507, 238–242, doi:10.1038/nature12956 (2014). [PubMed: 24487620]
31. Chen TW et al. Ultrasensitive fluorescent proteins for imaging neuronal activity. Nature 499, 295–300, doi:10.1038/nature12354 (2013). [PubMed: 23868258]
32. Zhang F et al. Optogenetic interrogation of neural circuits: technology for probing mammalian brain structures. Nature protocols 5, 439–456, doi:10.1038/nprot.2009.226 (2010). [PubMed: 20203662]

33. Ung K & Arenkiel BR Fiber-optic implantation for chronic optogenetic stimulation of brain tissue. Journal of visualized experiments : JoVE, e50004, doi:10.3791/50004 (2012). [PubMed: 23128465]
34. Armbruster BN, Li X, Pausch MH, Herlitze S & Roth BL Evolving the lock to fit the key to create a family of G protein-coupled receptors potently activated by an inert ligand. Proceedings of the National Academy of Sciences of the United States of America 104, 5163–5168, doi:10.1073/pnas.0700293104 (2007). [PubMed: 17360345]
35. Pankevich DE, Baum MJ & Cherry JA Olfactory sex discrimination persists, whereas the preference for urinary odorants from estrous females disappears in male mice after vomeronasal organ removal. The Journal of neuroscience : the official journal of the Society for Neuroscience 24, 9451–9457, doi:10.1523/JNEUROSCI.2376-04.2004 (2004). [PubMed: 15496681]
36. McClure C, Cole KL, Wulff P, Klugmann M & Murray AJ Production and titering of recombinant adeno-associated viral vectors. Journal of visualized experiments : JoVE, e3348, doi:10.3791/3348 (2011). [PubMed: 22143312]
37. Paxinos G & Franklin KB J. The mouse brain in stereotaxic coordinates, 2nd edition. Elsevier/Academic Press (2004).
38. Gunaydin LA et al. Natural neural projection dynamics underlying social behavior. Cell 157, 1535–1551, doi:10.1016/j.cell.2014.05.017 (2014). [PubMed: 24949967]
39. Byers SL, Wiles MV, Dunn SL & Taft RA Mouse estrous cycle identification tool and images. PloS one 7, e35538, doi:10.1371/journal.pone.0035538 (2012). [PubMed: 22514749]
40. Bankhead P et al. QuPath: Open source software for digital pathology image analysis. Scientific reports 7, 16878, doi:10.1038/s41598-017-17204-5 (2017). [PubMed: 29203879]
41. Cantu DA et al. EZcalcium: Open-Source Toolbox for Analysis of Calcium Imaging Data. Frontiers in neural circuits 14, 25, doi:10.3389/fncir.2020.00025 (2020). [PubMed: 32499682]
42. Chan KY et al. Engineered AAVs for efficient noninvasive gene delivery to the central and peripheral nervous systems. Nature neuroscience 20, 1172–1179, doi:10.1038/nn.4593 (2017). [PubMed: 28671695]
43. Heiman M, Kulicke R, Fenster RJ, Greengard P & Heintz N Cell type-specific mRNA purification by translating ribosome affinity purification (TRAP). Nature protocols 9, 1282–1291, doi:10.1038/nprot.2014.085 (2014). [PubMed: 24810037]
44. Love MI, Huber W & Anders S Moderated estimation of fold change and dispersion for RNA-seq data with DESeq2. Genome biology 15, 550, doi:10.1186/s13059-014-0550-8 (2014). [PubMed: 25516281]
45. Hornung V et al. 5'-Triphosphate RNA is the ligand for RIG-I. Science 314, 994–997, doi:10.1126/science.1132505 (2006). [PubMed: 17038590]
46. Huang KW & Sabatini BL Single-Cell Analysis of Neuroinflammatory Responses Following Intracranial Injection of G-Deleted Rabies Viruses. Frontiers in cellular neuroscience 14, 65, doi:10.3389/fncel.2020.00065 (2020). [PubMed: 32265666]
47. Chen EY et al. Enrichr: interactive and collaborative HTML5 gene list enrichment analysis tool. BMC bioinformatics 14, 128, doi:10.1186/1471-2105-14-128 (2013). [PubMed: 23586463]
48. Kuleshov MV et al. Enrichr: a comprehensive gene set enrichment analysis web server 2016 update. Nucleic acids research 44, W90–97, doi:10.1093/nar/gkw377 (2016). [PubMed: 27141961]
49. Choe HK et al. Oxytocin Mediates Entrainment of Sensory Stimuli to Social Cues of Opposing Valence. Neuron 87, 152–163, doi:10.1016/j.neuron.2015.06.022 (2015). [PubMed: 26139372]

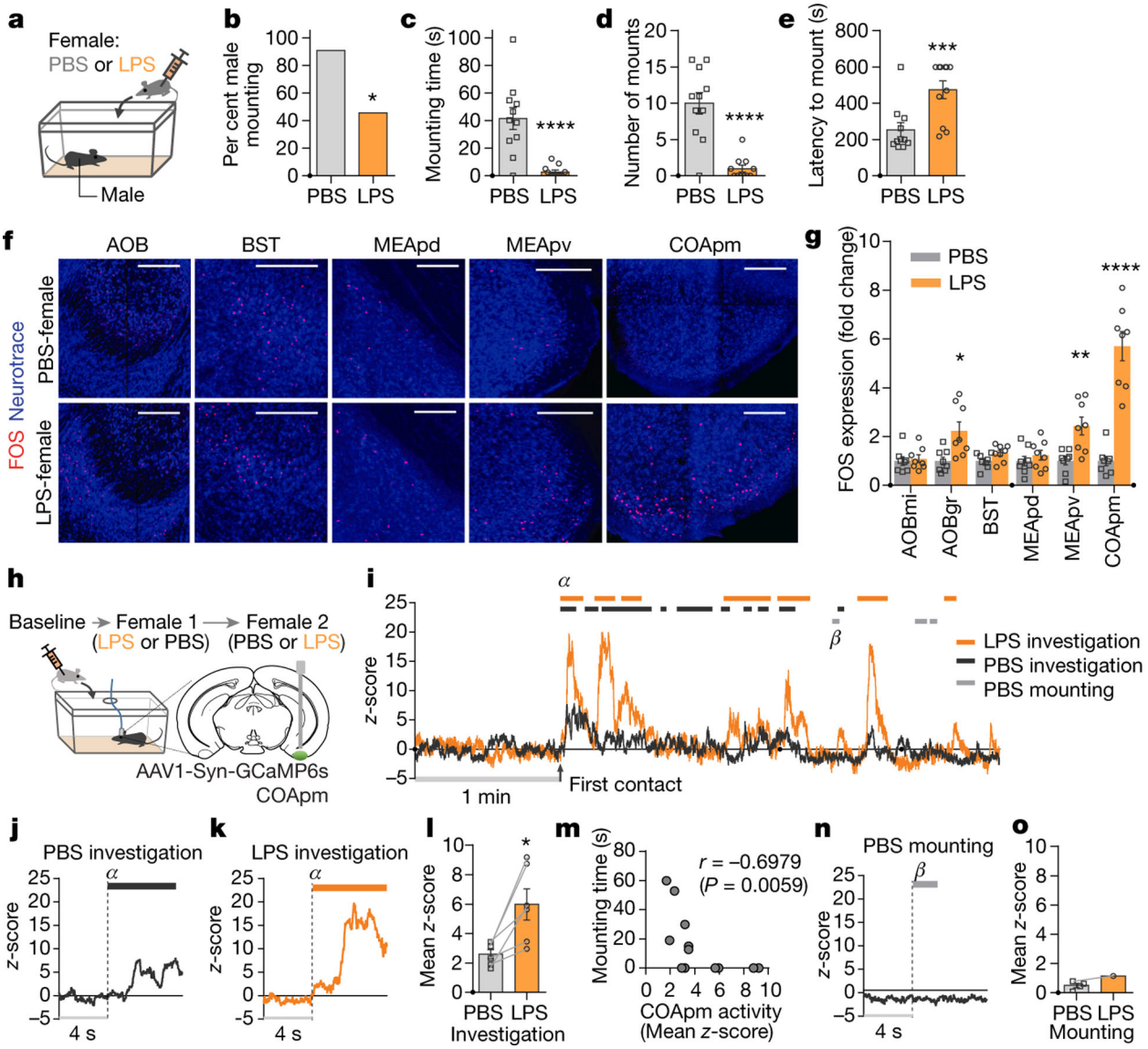

Figure 1. COApm is activated by LPS-treated females.

a-e, Male mounting behaviors towards a PBS- or LPS-treated female. Percentage of males engaged in mounting behavior (percent male mounting) (**b**), total duration of mounting bouts (mounting time) (**c**), number of mounting attempts (number of mounts) (**d**) and latency to the first mounting attempt (latency to mount) (**e**) during a 10-min test (PBS, n=11 and LPS, n=11; from 2 independent experiments). **f,g** Representative images of FOS expression in the vomeronasal pathway after interaction with PBS- or LPS-females (**f**) and fold change in the number of FOS-expressing neurons normalized to the mean of the PBS-female group for each region (**g**) (PBS, n=8 and LPS, n=8; from 2 independent experiments). Scale bar=200μm. AOBmi: mitral layer of the accessory olfactory bulb, AOBgr: granular layer of the accessory olfactory bulb, BST: bed nucleus of the stria terminalis, MEApd: posterodorsal part of the medial amygdalar nucleus, MEApv: posteroventral part of the medial amygdalar nucleus. **h-o,** Virus encoding GCaMP6s (AAV_1-Syn-GCaMP6s) was targeted to the COApm for fiber photometry recordings. Male mice were sequentially presented with a PBS- or LPS-

female in counterbalanced sessions (**h**). Representative trace of COApm bulk fluorescence signal during interactions with the PBS- (black) or LPS-female (orange) (**i**). Representative traces (marked as α in (i)) (**j, k**) and the average mean z-score of the fluorescence during direct investigation of the PBS- or LPS-female (**l**). Spearman's correlation between mean z-score during investigation and mounting time. Data are pulled from the sessions with PBS- and LPS-females (**m**). Representative trace (marked as β in (i)) (**n**) and the average mean z-score of the fluorescence during mounting of the PBS- or LPS-female (**o**) (n=6 from 3 independent experiments). *P<0.05, **P<0.01, ***P<0.001 and ****P<0.0001 calculated by Chi-Square Test of Independence (**b**), unpaired two-tailed t-test (**c-e**), two-way ANOVA with Sidak's post-hoc test (**g)** and paired two-tailed t-test (**l**). Graphs indicate mean ± s.e.m. p-values are described in the supplementary statistical information file.

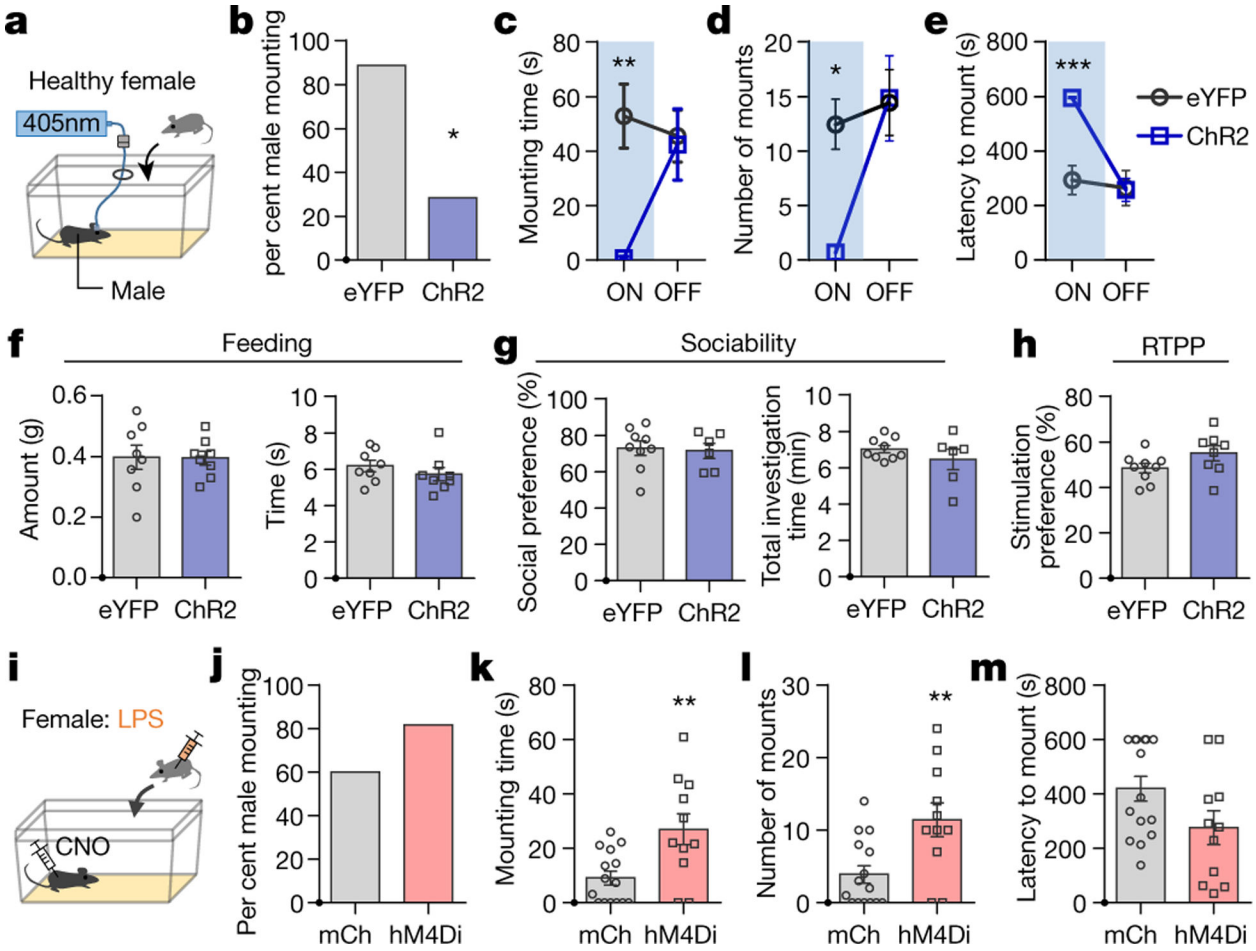

Figure 2. COApm mediates suppression of mating behaviors towards unhealthy females.

a-e, Male mice expressing EYFP (AAV_2-hSyn-EYFP) or channelrhodopsin (ChR2, AAV_2-hSyn-hChR2-EYFP) in COApm were tested for mating behaviors towards healthy females in the presence (ON) or absence (OFF) of COApm photoactivation. Percent male mounting (**b**), mounting time (**c**), number of mounts (**d**), and latency to mount (**e**) (EYFP, n=9 and ChR2, n=7; from 2 independent experiments). **f,** Total amount of food eaten and time spent eating used to assess feeding behavior during COApm photoactivation (EYFP, n=8 and ChR2, n=8; from 2 independent experiments). **g,** Social preference (time spent investigating a social object/total time spent investigating social and inanimate objects) and total investigation time measured during a sociability test with COApm photoactivation (EYFP, n=9 and ChR2, n=6; from 2 independent experiments). **h,** Stimulation preference (time spent in the compartment where photoactivation occurs/total testing time) during a real-time place preference (RTPP) test (EYFP, n=9 and ChR2, n=8; from 2 independent experiments). **i-m,** Male mice expressing mCherry (AAV_2-hSyn-mCherry) or inhibitory DREADD (hM4Di, AAV_2-hSyn-hM4D(Gi)-mCherry) in COApm were injected with Clozapine-N-Oxide (CNO) and tested for mating behaviors towards LPS-females (**i**). Percent male mounting (**j**), mounting time (**k**), number of mounts (**l**), and latency to mount (**m**) (mCherry, n=15 and hM4Di, n=11; from 3 independent experiments). *P<0.05, **P<0.01 and ***P<0.001 calculated by Chi-Square Test of Independence (**b**), two-way repeated measures ANOVA

with Bonferroni's post-hoc test (**c-e**) and unpaired two-tailed *t*-test (**k**, **l**). Graphs indicate mean ± s.e.m. p-values are described in the supplementary statistical information file.

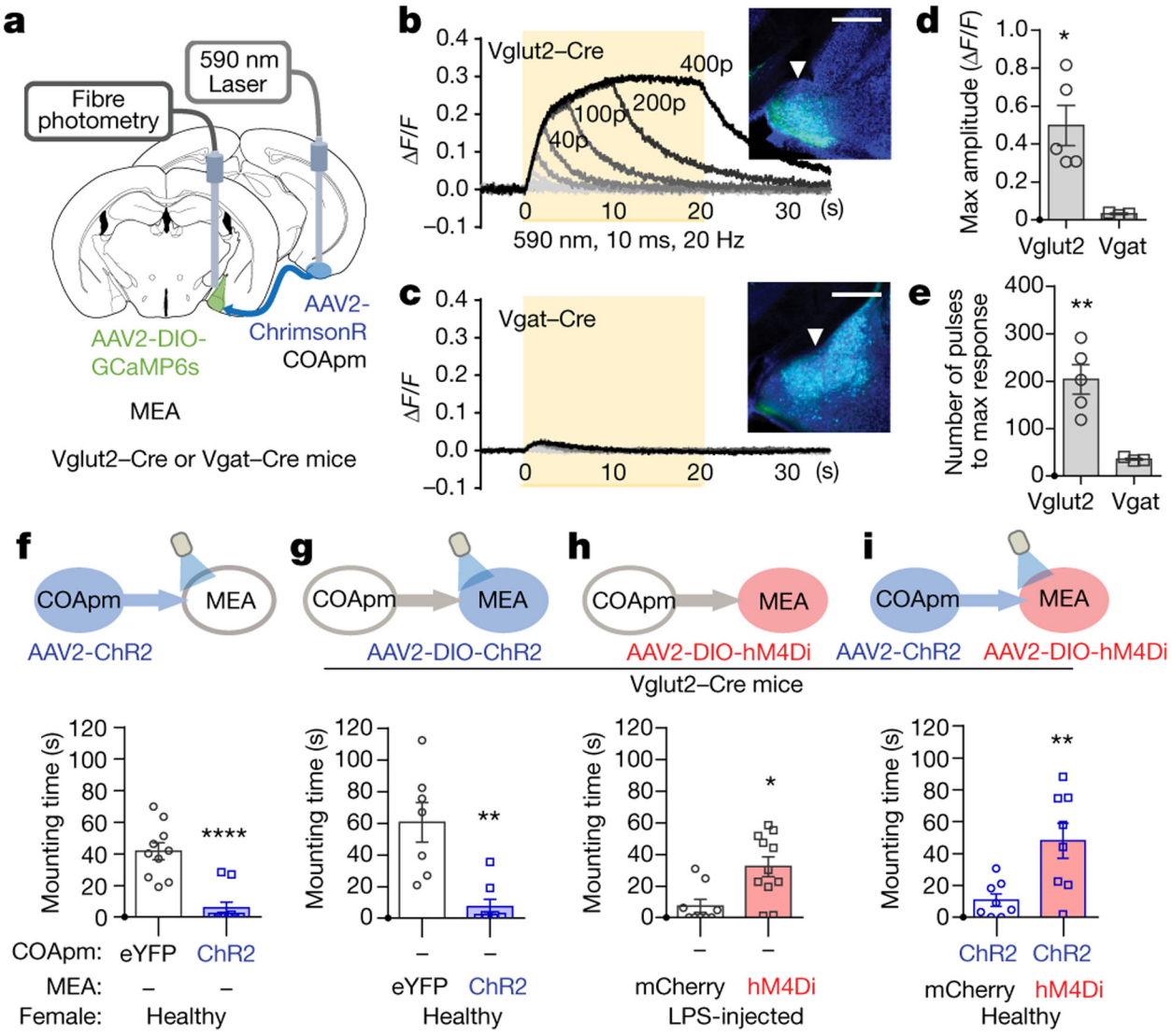

Figure 3. COApm projections to MEA-Vglut2(+) neurons mediate suppression of mating towards LPS-females.

a-e, Red-shifted opsin ChrimsonR (AAV_2-hSyn-ChrimsonR-tdTomato) was expressed in COApm, while GCaMP6s was expressed in MEA for fiber photometry analyses. Bulk fluorescence signal upon COApm photoactivation was measured in either MEA-Vglut2(+) or MEA-Vgat(+) neurons. Representative traces of changes in fluorescence signal in MEA upon photoactivation of COApm using light trains with 1, 5, 10, 20, 40, 100, 200 and 400 pulses, respectively. Inset images show GCaMP6s expression in MEA-Vglut2(+) or MEA-Vgat(+) neurons. Arrowheads indicate the placement of the optic fiber for fiber photometry (**b,c**). Maximum amplitude evoked by photoactivation of COApm with 400 pulses of light (**d**) and number of light pulses to reach max amplitude (**e**) (Vglut2-Cre, n=5 and Vgat-Cre, *n*=3; from 3 independent experiments). Scale bar=500μm. **f-i,** Quantification of male mounting behaviors during concurrent manipulation of COApm-MEA axonal projections and MEA-Vglut2(+) neurons. Male subjects were wild type for (f) or Vglut2-Cre mice for (g, h and i). Female subjects were healthy for (f, g and i) or LPS-injected for

(h). **f,** Mounting time with photoactivation of COApm-MEA projections (EYFP, n=10 and ChR2, n=10; from 2 independent experiments). **g,** Mounting time with photoactivation of MEA-Vglut2(+) neurons (EYFP, n=7 and ChR2, n=8; from 2 independent experiments). **h,** Mounting time towards LPS-females with hM4Di-inhibition of MEA-Vglut2(+) neurons (mCherry, n=9 and hM4Di, n=11; from 2 independent experiments). **i,** Mounting time with concurrent photoactivation of COApm-MEA projections and hM4Di-inhibition of MEA-Vglut2(+) neurons (mCherry, n=8 and hM4Di, n=8; from 2 independent experiments). *P<0.05, **P<0.01 and ****P<0.0001 calculated by unpaired two-tailed t-test. Graphs indicate mean ± s.e.m. p-values are described in the supplementary statistical information file.

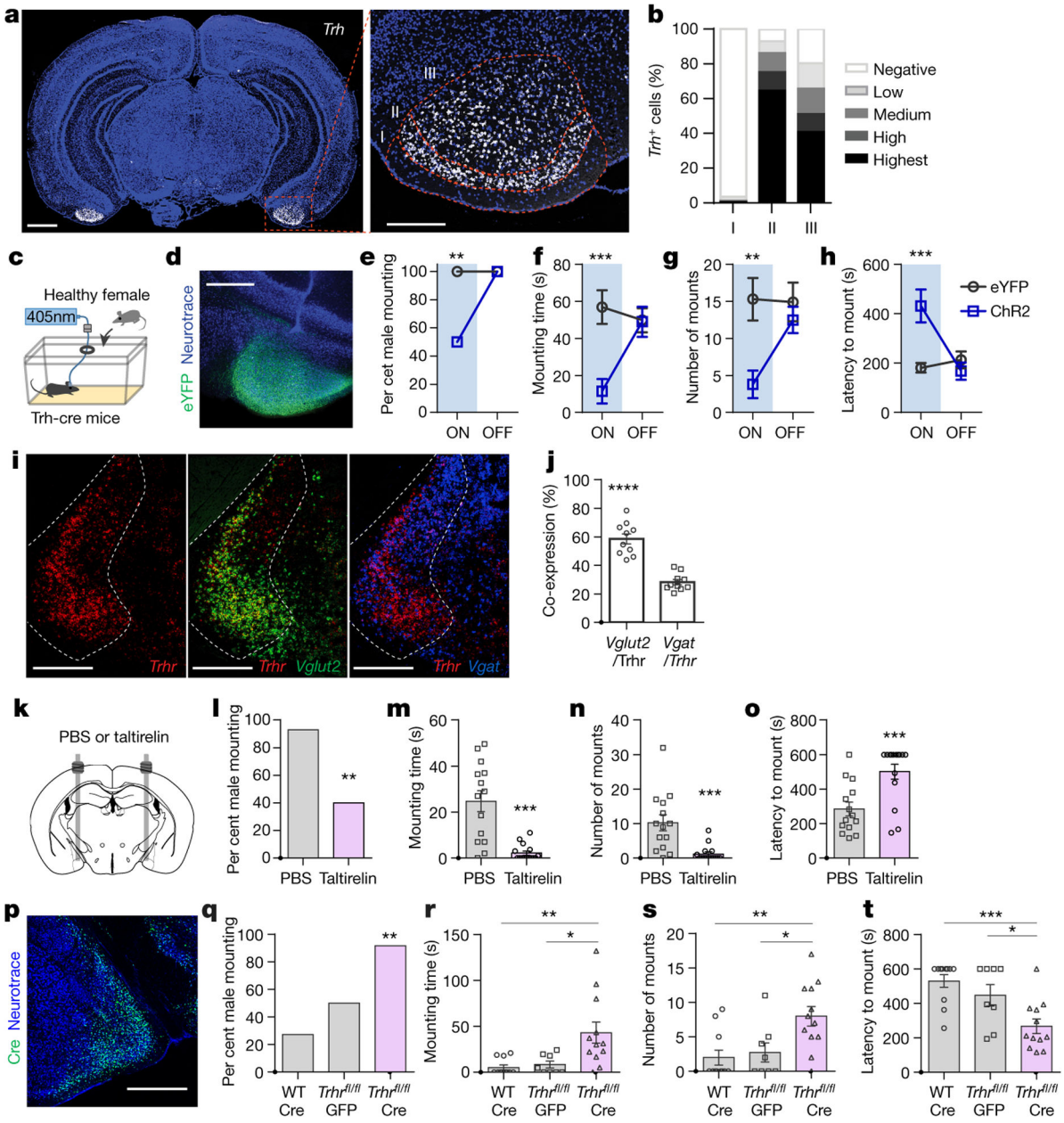

Figure 4. Suppression of social behaviors engages COApm-TRH(+) neurons.

a,b, Representative image (**a**) and quantification (**b**) of *Trh* mRNA expression in wild-type mice at anterior-posterior (AP) −2.9 mm according to cortical layers (n=13 sections from 4 mice; from 2 independent experiments). Dotted line defines cortical layers I, II, and III. Scale bar=1mm (left) and 300μm (right). **c-h**, Trh-Cre male mice expressing EYFP (AAV_2-hSyn-DIO-EYFP) or ChR2 (AAV_2-hSyn-DIO-hChR2-EYFP) in COApm-TRH(+) neurons were tested for mating behaviors towards healthy females in the presence (ON) or absence (OFF) of photoactivation (**c**). Representative image of ChR2 expression in COApm (**d**). Percent male mounting (**e**), mounting time (**f**), number of mounts (**g**), and latency to mount (**h**) (EYFP, n=13 and ChR2, n=10; from 2 independent experiments). Scale bar=500μm. **i,j,** Representative images (**i**) and quantification (**j**) of the overlap between cells expressing

Trhr (red), *Vglut2* (green) and *Vgat* (blue) mRNA in MEA of wild-type mice at AP −1.8 mm (n=10 MEA sections from total 5 mice; from 4 independent experiments). Dotted line indicates MEA. Scale bar=500μm. **k-o,** TRH analog taltirelin was bilaterally injected into MEA (**k**). Percent male mounting (**l**), mounting time (**m**), number of mounts (**n**), and latency to mount (**o**) (PBS, n=14 and Taltirelin, n=15; from 2 independent experiments). **p-t,** Wild-type (WT) or $TRHR^{fl/fl}$ male mice expressing GFP (AAV_1-hSyn-GFP) or Cre (AAV_1-Syn-Cre) in the MEA were tested for mating behaviors towards LPS-females. Representative image of Cre expression in MEA (**p**). Percent male mounting (**q**), mounting time (**r**), number of mounts (**s**), and latency to mount (**t**) (WT:Cre, n=11; $TRHR^{fl/fl}$:EYFP, n=8 and $TRHR^{fl/fl}$:Cre, n=12; from 2 independent experiments). Scale bar= 500μm. *P<0.05, **P<0.01, ***P<0.001 and ****P<0.0001 calculated by Chi-Square Test of Independence (**e,l,q**), two-way repeated measures ANOVA with Bonferroni's post-hoc test (**f-h**) and paired two-tailed t-test (**j**), unpaired two-tailed t-test (**m-o**) and one-way ANOVA with Bonferroni's post-hoc test (**r-t**). Graphs indicate mean ± s.e.m. p-values are described in the supplementary statistical information file.